



Published in final edited form as:

Cell Rep. 2022 July 12; 40(2): 111039. doi:10.1016/j.celrep.2022.111039.

A specialized Hsp90 co-chaperone network regulates steroid hormone receptor response to ligand

Sarah J. Backe^{1,2,3}, **Rebecca A. Sager**^{1,3}, **Bethany R. Regan**^{1,3,4}, **Julian Sit**^{1,3,4}, **Lauren A. Major**^{1,3,4}, **Gennady Bratslavsky**^{1,2,3}, **Mark R. Woodford**^{1,2,3}, **Dimitra Bourboulia**^{1,2,3}, **Mehdi Mollapour**^{1,2,3,5,6,*}

¹Department of Urology, SUNY Upstate Medical University, Syracuse, NY 13210, USA

²Department of Biochemistry and Molecular Biology, SUNY Upstate Medical University, Syracuse, NY 13210, USA

³Upstate Cancer Center, SUNY Upstate Medical University, Syracuse, NY 13210, USA

⁴College of Medicine, SUNY Upstate Medical University, Syracuse, NY 13210, USA

⁵Twitter: @medmol

⁶Lead contact

SUMMARY

Heat shock protein-90 (Hsp90) chaperone machinery is involved in the stability and activity of its client proteins. The chaperone function of Hsp90 is regulated by co-chaperones and post-translational modifications. Although structural evidence exists for Hsp90 interaction with clients, our understanding of the impact of Hsp90 chaperone function toward client activity in cells remains elusive. Here, we dissect the impact of recently identified higher eukaryotic co-chaperones, FNIP1/2 (FNIPs) and Tsc1, toward Hsp90 client activity. Our data show that Tsc1 and FNIP2 form mutually exclusive complexes with FNIP1, and that unlike Tsc1, FNIP1/2 interact with the catalytic residue of Hsp90. Functionally, these co-chaperone complexes increase the affinity of the steroid hormone receptors glucocorticoid receptor and estrogen receptor to their ligands *in vivo*. We provide a model for the responsiveness of the steroid hormone receptor activation upon ligand binding as a consequence of their association with specific Hsp90:co-chaperone subpopulations.

Graphical Abstract

This is an open access article under the CC BY-NC-ND license (<http://creativecommons.org/licenses/by-nc-nd/4.0/>).

*Correspondence: mollapom@upstate.edu.

AUTHOR CONTRIBUTIONS

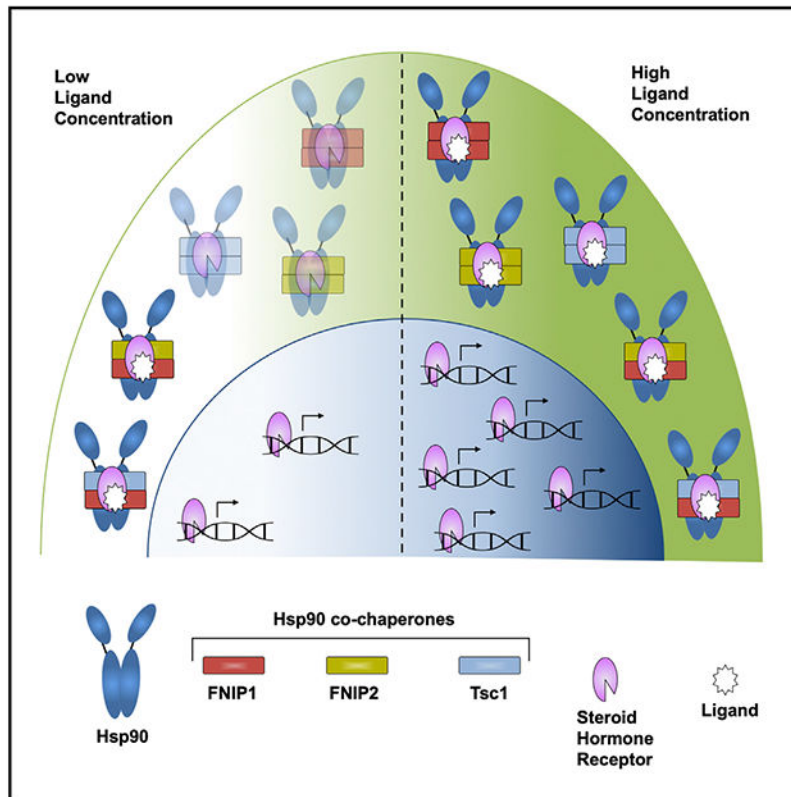
S.J.B., M.R.W., R.A.S., B.R.R., J.S., L.A.M., and M.M. performed experiments. S.J.B., M.R.W., R.A.S., G.B., D.B., and M.M. designed experiments. S.J.B., M.R.W., and M.M. wrote the manuscript. M.M. conceived the project.

SUPPLEMENTAL INFORMATION

Supplemental information can be found online at <https://doi.org/10.1016/j.celrep.2022.111039>.

DECLARATION OF INTERESTS

The authors declare no competing interests.



In brief

Backe et al. demonstrate that responsiveness of the steroid hormone receptors upon ligand-binding-mediated activation depends on their association with specific Hsp90:co-chaperone (FNIP1, FNIP2, and Tsc1) subpopulations. This study reveals that formation of different Hsp90:co-chaperone:client complexes provide differentially primed pools of client proteins ready to act in different cellular environments.

INTRODUCTION

Heat shock protein-90 (Hsp90) is a molecular chaperone responsible for maintaining the stability and activity of a large and disparate set of proteins, termed clients (Schopf et al., 2017). Due to the quantity and diversity of its clients, Hsp90 has been nicknamed “guardian of the proteome.” The Picard lab maintains an updated list of Hsp90 clients (<https://www.picard.ch/downloads/Hsp90interactors.pdf>) including kinases and transcription factors (Taipale et al., 2012; Tang et al., 2022), as well as all steroid hormone receptors (SHRs). The capacity of Hsp90 to chaperone its approximately 300 client proteins is strictly dependent on its ATP hydrolysis activity (Biebl and Buchner, 2019; Panaretou et al., 2002; Prodromou, 2012). Hsp90 functions as a dimer, in which each protomer can be subdivided into three distinct domains (Ali et al., 2006; Verba et al., 2016). The amino-terminal domain (NTD) contains the ATP-binding pocket (Prodromou et al., 1997). A highly charged and flexible linker connects the NTD to the middle domain (MD) (Hainzl et al., 2009; Tsutsumi

et al., 2012), and the carboxy-terminal domain (CTD) provides the dimerization interface (Harris et al., 2004; Prodromou and Pearl, 2003; Weikl et al., 2000).

Proteins termed co-chaperones regulate various aspects of Hsp90 chaperone function including rate of ATP hydrolysis and client recruitment and loading onto the chaperone machinery (Biebl et al., 2020; Cox and Johnson, 2011; Eisele et al., 2021). Of the ~25 co-chaperones described to date, a set of core co-chaperones that are essential for client maturation in yeast have been identified (Dean and Johnson, 2021; Sahasrabudhe et al., 2017). While most of these co-chaperones have a human ortholog, whether the essential complement of core co-chaperones is strictly conserved in humans remains unknown.

Our lab has identified three new co-chaperones (FNIP1, FNIP2, and Tsc1) exclusive to high eukaryotes that function as client scaffolds to load both kinase and non-kinase clients onto Hsp90 (Woodford et al., 2016, 2017). We found several similarities in the observed functions of the FNIPs and Tsc1 as Hsp90 co-chaperones. All three co-chaperones decelerated Hsp90 ATPase activity and were required for the stability of Hsp90 clients such as glucocorticoid receptor (GR), folliculin (FLCN), Cdk4, and Raf (Woodford et al., 2016, 2017). Additionally, FNIP1 and Tsc1 displayed similar mechanisms for binding to Hsp90, and all three co-chaperones competed for binding to Hsp90 with the activating co-chaperone Aha1. Furthermore, FNIP1, FNIP2, and Tsc1 all enhanced Hsp90 binding to ATP and the ATP-competitive inhibitor ganetespib (GB). Furthermore, we have shown that Tsc1 can compensate for FNIP1 to scaffold FLCN to Hsp90 under certain cellular conditions (Sager et al., 2018); however, it is unclear whether these proteins act antagonistically, cooperatively, or independently.

SHRs are a well-described class of Hsp90 clients whose stability and activity are highly dependent on the chaperone machinery. Work led largely by Pratt and Toft has contributed extensively to our understanding of SHR chaperoning by molecular chaperones (Bresnick et al., 1988, 1989; Dittmar et al., 1997; Fang et al., 1996; Johnson and Toft, 1994; Picard et al., 1990; Pratt, 1987; Pratt et al., 1992; Pratt and Toft, 2003). The current model of GR maturation describes a process in which Hsp70 first binds to GR, unfolding a portion of the GR ligand-binding domain (LBD) and is subsequently passed to Hsp90 for final maturation by an adaptor co-chaperone, Hsp70-Hsp90 organizing protein (Hop) (Chen et al., 1996; Chen and Smith, 1998; Kirschke et al., 2014; Lorenz et al., 2014; Moessmer et al., 2022). However, the mechanism by which Hsp90 primes its clients, including GR, for activation is unresolved.

Here, we show that the co-chaperones FNIP1, FNIP2, and Tsc1 enhance SHR activity by increasing affinity for ligand. Fine-tuning of SHR ligand affinity and activity is increasingly relevant, as ligand-competitive inhibitors are under investigation in cancer and other diseases (Abdou et al., 2008; Crawford et al., 2018; Koorneef et al., 2020; Sharma et al., 2018). Furthermore, in many cases, cancers become resistant to hormone therapy, highlighting the importance of understanding the mechanisms of resistance and potential pathways to bypass such resistance.

RESULTS

Hsp90 catalytic loop facilitates binding of Tsc1 and FNIPs co-chaperones

We have recently identified FNIP1/2 and Tsc1 as decelerators of the Hsp90 chaperone machinery (Sager et al., 2019; Woodford et al., 2016, 2017); however, a mechanistic understanding of this regulation remains elusive. Here, we immunoprecipitated FNIP1, FNIP2, and Tsc1 with the goal of identifying a global interactome by mass spectrometry (Figure 1A; Table S1). We identified 20 proteins that interacted with both FNIP1 and Tsc1, 11 proteins that interacted only with Tsc1, and 34 proteins that were specific for FNIP1. Notably, FNIP2 shared only three interactors with FNIP1 and two with Tsc1. We confirmed interaction between selected endogenous proteins by immunoblot (Figures S1A and S1B). One of the key findings of this experiment was the presence of reciprocal Tsc1 and FNIP1 interaction; however, FNIP2 was notably absent. We confirmed this finding by immunoprecipitation (IP) of FNIP1- and FNIP2-HA and coIP of endogenous Tsc1 (Figure 1B). The reciprocal IP of Tsc1-FLAG provided similar data (Figure 1C). While FNIP1 and Tsc1 were consistently found in complex together, FNIP2 and Tsc1 did not interact.

Hsp90 chaperone activity is coupled to conformational changes directed by its ability to hydrolyze ATP. These include “open” and “closed” states of Hsp90, which can be mimicked by point mutations in the ATP-binding domain (Panaretou et al., 1998). Previous work from our group showed preferential binding of Tsc1 to the Hsp90 α -E47A mutant, which promotes the closed conformation of Hsp90 (Woodford et al., 2017). Both FNIP1 and FNIP2 also preferred binding to this closed conformation mutant (Figures S2A and S2B). Our work has previously shown that FNIP1/2 and Tsc1 compete with the accelerator of Hsp90 ATPase activity (Aha1) for binding to Hsp90 (Woodford et al., 2017). Hsp90 α -V411 is required for Aha1 binding to Hsp90 (Meyer et al., 2004), so we utilized the previously established Hsp90 α -V411E mutant to evaluate whether FNIP1/2 occupy a similar binding surface. Our data showed that, as expected, interaction of Tsc1 with Hsp90 is abrogated (Figure 1D). We did not, however, obtain similar data with FNIP1 and FNIP2, suggesting a distinct Hsp90 interaction surface compared with Tsc1 (Figure 1D).

Given that these co-chaperones bind to the middle domain (MD) and impact Hsp90 activity, we tested whether deletion of the Hsp90 catalytic domain impacted the binding of FNIP1/2 and Tsc1 to Hsp90. Interestingly, FNIP1 and FNIP2 displayed a marked increase in binding to Hsp90 lacking its catalytic loop (CAT) (Figure 1E); however, Tsc1 interaction was unaffected. In order to identify key residues in Hsp90 potentially involved in interaction with FNIPs and Tsc1, we made a series of mutations within the catalytic domain of Hsp90 (Figure 1F). Our data show that the catalytic residue R399A mutant as well as Q403A abrogated interaction with both FNIPs and Tsc1 while demonstrating stronger binding to Aha1 when compared with the wild-type (WT)-Hsp90 (Figures 1G and S2C). Looking at the overall pattern of interaction, FNIP1 and Tsc1 show similar binding with respect to the Hsp90 catalytic domain mutants; however, this pattern is distinct from that of FNIP2 (Figures 1G and S2C). Taken together, our data show that Tsc1 interacts exclusively with FNIP1 and that FNIP1/2 and Tsc1 utilize unique strategies for Hsp90 interaction.

Architecture of FNIP2 co-chaperone association with Hsp90

Previous work has dissected FNIP1 and Tsc1 interaction with Hsp90 in detail, identifying the C terminus of FNIP1 (FNIP1-D) and Tsc1 (Tsc1-D) as the critical Hsp90-binding element (Baba et al., 2006; Huang and Manning, 2008; Woodford et al., 2016, 2017) (Figure 2A). However, it is unknown whether the FNIP2 co-chaperone employs a similar binding strategy to Hsp90. Using a similar truncation strategy (Hasumi et al., 2008; Woodford et al., 2016), we identified the FNIP2 N terminus (aa 1–584; FNIP2-AB) as necessary for Hsp90 binding (Figure 2B). Attempts to divide this region further resulted in a loss of binding, though the extreme N terminus (aa 1–281; FNIP2-A) retained some ability to interact with Hsp90 (Figure 2C). We have previously shown that full-length FNIP2 prefers binding to the MD of Hsp90 (Woodford et al., 2016). Interestingly, while FNIP2-AB bound weakly to the Hsp90 MD, it demonstrated a marked preference for the Hsp90 C domain (Figure 2D). Some Hsp90 co-chaperones (HOP, PP5, FKBP51/52, and Cpr6) possess a tetratricopeptide repeat domain (TPR) that facilitates interaction with Hsp90 via its C-terminal MEEVD extension. Though we did not identify any predicted TPR domains in FNIP1/2, we assayed their requirement for Hsp90-MEEVD. Perhaps unsurprisingly, interaction of FNIP1/2 was independent of this Hsp90 binding motif (Figures S3A and S3B).

FNIP1 and FNIP2 have previously been reported to homo- and heterodimerize (Hasumi et al., 2008; Woodford et al., 2016). Additionally, we have shown that the D fragment of FNIP1 also forms a homodimer (Figure 2E), leading us to ask whether these two Hsp90-binding fragments also exist in the same complex. Our data show that the Hsp90-binding components of these co-chaperones (FNIP1-D, FNIP2-AB) interact in cells (Figure 2F), suggesting that the C domain (D fragment) of FNIP1 and the N domain of FNIP2 (AB fragment) are sufficient to form a complex with Hsp90. This interaction is represented schematically in Figure 2G. Given that FNIP1 and Tsc1 also interact in cells (Figures 1A–1C), we next asked if the Hsp90-binding domains were sufficient to mediate interaction between FNIP1 and Tsc1. Our data show that FNIP1-D and Tsc1-D domains interact in cells (Figure 2H). Taken together, our data demonstrate that despite a high degree of sequence similarity, FNIP1/2 utilize distinct strategies to interact with Hsp90.

Differential regulation of client protein activity by FNIPs and Tsc1 co-chaperones

We have previously shown that FNIPs and Tsc1 regulate the chaperoning of Hsp90 client proteins (Sager et al., 2019; Woodford et al., 2016, 2017); however, the combinatorial impact of these co-chaperones toward kinase and non-kinase clients remained unknown. Here, we utilized baker's yeast *S. cerevisiae* expressing human Hsp90 α as the sole copy of Hsp90 (Mollapour et al., 2010). As *S. cerevisiae* does not have true FNIP and Tsc1 orthologs, we were able to express these co-chaperones alone and in combination to assess their impact on *bona fide* Hsp90 clients. Our data show that expression of FNIP1 and FNIP2, individually and in combination, enhances the activity of the kinase clients v-Src (Nathan and Lindquist, 1995) and Slf2 (Truman et al., 2006) (measured by RLM1-*lacZ* reporter) (Figures 3A and 3B; Table S2). Conversely, expression of Tsc1 in yeast negatively impacts the activity of these two kinases, while expression of FNIP2 compensates for this Tsc1-mediated suppression (Figures 3A and 3B). Additionally, expression of FNIP1 in

combination with Tsc1 greatly enhanced kinase client stability and activity compared with Tsc1 alone (Figures 3A and 3B).

Previous work has shown that heat shock factor (HSF1) is also an Hsp90 client (Zou et al., 1998). We used heat shock element *lacZ* (HSE-*lacZ*) reporter in order to evaluate the impact of FNIPs and Tsc1 toward HSF1 activity. Expression of FNIPs and Tsc1 alone leads to elevated HSF1 activity, even in the absence of heat-shock stress (Figure 3C). Interestingly, this effect was further elevated upon expression of these co-chaperones in combination, as well as with heat stress (Figure 3C). Collectively, our data suggest that cooperative action of these co-chaperones attunes the stability and activity of Hsp90 client proteins (Figure 3D).

FNIPs and Tsc1 co-chaperones enhance the activity and ligand binding of SHRs

Hsp90 chaperones SHRs such as GR, androgen receptor (AR), and estrogen receptor (ER α) (Binart et al., 1995; Bresnick et al., 1988; Fang et al., 1996). We have previously shown that FNIPs and Tsc1 impact the stability of GR (Woodford et al., 2016, 2017). However, the effect of these co-chaperones toward SHR activity and ligand binding remained elusive. Here, we expressed FNIPs and Tsc1 individually and in combination in *S. cerevisiae* expressing GR and human Hsp90 α as the sole copy of Hsp90. Our data show that FNIPs and Tsc1 enhanced GR activity in cells (Figure 4A). Interestingly, combinatorial expression of FNIP1/FNIP2, FNIP1/Tsc1, and FNIP2/Tsc1 further enhanced the activity of GR (Figure 4A). We made similar observations with regards to the impact of FNIPs/Tsc1 on the activity of AR (Figure 4B) and ER α (Figure 4C). Taken together, our data suggest that Tsc1 expression significantly increased SHR activity in combination with either FNIP1 or FNIP2 when compared with FNIP1/FNIP2 (Figures 4A–4D).

We next examined whether expression of these co-chaperones affects GR binding to its ligand (dexamethasone). We expressed FNIPs and Tsc1 co-chaperones both alone and in combination in yeast that expresses GR (Figure S4A) and challenged the cell lysate with increasing amounts of biotinylated dexamethasone (Figure 4E). Although our data show that GR is capable of binding to dexamethasone in the absence of FNIPs and Tsc1, expression of these co-chaperones increases the affinity of GR for its ligand (Figure 4E). Furthermore, combination expression of FNIP1/FNIP2, FNIP1/Tsc1, and FNIP2/Tsc1 further increased GR binding to dexamethasone (Figure 4E). These data reflect our earlier observation of increased GR activity. Additionally, our data demonstrated that combined expression of FNIP1/FNIP2, FNIP1/Tsc1, and FNIP2/Tsc1 enhanced ER α binding to its ligand (β -estradiol-biotin) (Figures 4F, 4G, and S4B). Taken together, FNIPs and Tsc1 enhance GR and ER α binding to their ligands and, consequently, stimulate their activity.

Hsp90 induces conformational alterations in GR LBD

Previous work has shown that Hsp90 binds to the GR LBD (Simons et al., 1989); however, the structural interaction of FNIPs and Tsc1 co-chaperones in this complex remains elusive. We initially co-expressed FNIP1-HA with different functional domains of GR-FLAG (Figure 5A) in HEK293 cells and showed that FNIP1 and FNIP2 interact with both the ligand and DNA-binding domains (Figures 5B and 5C). Surprisingly, Tsc1 interacted exclusively with the LBD of GR (Figure 5D).

Since our findings clearly demonstrate that the Hsp90 chaperone machinery influences GR ligand binding, we dissected this process at the structural level. Molecular simulations of GR ligand binding and release highlighted three α helices (α -helix-3, -7, and -11) in the GR LBD that move to form a site for ligand entry and exit from the ligand-binding pocket (Figure 5E) (Edman et al., 2015). We used limited proteolysis-coupled mass spectrometry (LiP) analysis to determine the impact of Hsp90 and dexamethasone on the conformation of recombinant GR protein (Figure 5F; Table S3). We found that three peptides in the GR LBD lost protease sensitivity in at least one of the conditions. The region of D641-Y648, which connects α -helix-10 and -11, lost protease sensitivity in the presence of dexamethasone. Addition of Hsp90 α precluded protease sensitivity of the carboxy-end of α -helix-7 (I701-W712), which is important for positioning the ligand entry/exit pore. Notably, peptide S746-N759, which partially comprises the ligand-dependent transcriptional activation domain-2 (AF-2) (MacGregor and Jordan, 1998) in helix-12, lost protease sensitivity under both conditions. Collectively, our results show that the Hsp90:co-chaperone complex interacts with GR through the LBD and subsequently alters the LBD conformation.

DISCUSSION

Hsp90 is involved in maintaining the stability and activity of its client proteins. The chaperone function of Hsp90 is regulated by co-chaperones. However, it is unclear how specialized co-chaperones in higher eukaryotes, such as FNIPs and Tsc1, work in concert to regulate the activation of client proteins. Our previous work has shown that FNIPs and Tsc1 decelerate the ATPase activity of Hsp90 and behave as a scaffold for client protein binding to the chaperone machinery. Here, we provide evidence that FNIP2 amino-terminal domain (FNIP2-AB), contrary to FNIP1, binds to the carboxy-domain of Hsp90. These data confirm that these two co-chaperones are not functionally identical, as suggested by previous work (Hasumi et al., 2008). Our network analysis provided further evidence that FNIP1 and Tsc1 function in similar cellular pathways and interact with a largely overlapping set of proteins and, notably, each other. In contrast, FNIP2 and Tsc1 form mutually exclusive complexes with FNIP1 and Hsp90. It is noteworthy that FNIP1, FNIP2, and Tsc1 interactomes revealed additional hits involved in pathways such as transcription and chromatin remodeling that warrant further investigation.

This raises the question of what is the physiological benefit of these hetero-co-chaperone:Hsp90 complexes? Our data presented here suggest that the responsiveness of the SHR upon ligand binding depends on their association with the specific *in vivo* Hsp90:co-chaperone sub-populations, potentially allowing cells to fine-tune SHR response to varying agonist availability (Figure 6). Based on our data presented here, we propose that these co-chaperones, in complex with Hsp90, aid in the necessary repositioning of the C terminus of GR LBD, priming GR for ligand binding (Fang et al., 2006; Kaziales et al., 2021). Furthermore, these results suggest that levels of FNIPs and Tsc1 proteins may be useful biomarkers for determining patient responsiveness to hormone therapy. Mutation and inactivation of Tsc1 results in a multifaceted syndrome called tuberous sclerosis (TS) classified by tumors in different organs such as the skin, heart, lung, and kidneys. Patients with TS may be less likely to respond to hormone-derived drugs such as the ER agonists raloxifene and tamoxifen, which are commonly used to treat breast cancer. Further

understanding of the mechanism in which these co-chaperones enhance SHR ligand affinity will be critical to uncovering the precise translational application of the results presented here.

SHRs are a well-characterized class of Hsp90 clients, and previous works provide a compelling model for GR activation by Hsp90 *in vitro* (Kirschke et al., 2014; Lorenz et al., 2014; Murphy et al., 2003). Additionally, previous studies have also suggested that Hsp90 participates in the activation process by maintaining SHRs in a high-affinity ligand-binding conformation (Fang et al., 1996). Our results are in agreement with this; however, previous studies did not take into account the influence of highly specialized co-chaperones such as FNIPs and Tsc1 in eukaryotes. In this study, we took advantage of our previously established yeast system (Mollapour et al., 2010; Piper et al., 2003; Sager et al., 2019) and dissected the impact of these co-chaperones toward SHR activity and ligand binding. Our findings provide further evidence that FNIP1/2 together, as well as FNIP1/Tsc1, can form heterotrimeric complexes with Hsp90 and increase binding of SHRs, such as GR and ER α , to their ligands. FNIP2 and Tsc1 also form mutually exclusive complexes with Hsp90 and consequently increase SHR activity. Proteins that increase the transcriptional activity of SHR are generally termed “co-activators” and contain an “LxxLL” motif that interacts with the AF-2 domain of SHR (Heery et al., 1997; Savkur and Burris, 2004). Intriguingly, FNIP1, FNIP2, and Tsc1 all contain LxxLL motifs (FNIP1²⁶²LSSLL²⁶⁶; FNIP2²⁴⁵LSSLL²⁴⁹; Tsc1¹¹³LPSLL¹¹⁷), suggesting that these co-chaperones may be SHR co-activators. Interestingly, expression of Tsc1 with either FNIP1 or FNIP2 provides increased activation relative to FNIP-only combinations, despite our finding that FNIP2 and Tsc1 do not work in the same complex. This suggests that the FNIPs and Tsc1 have complementary, but not redundant, function toward client activation.

We have previously shown that knock down of FNIP1, FNIP2, or Tsc1 is detrimental to the stability of kinase and non-kinase clients. Surprisingly, over-expression of Tsc1 had a negative impact on kinase protein levels, whereas over-expression of FNIP1 or FNIP2 led to an increase in kinase client protein levels. This is in line with our findings here that Tsc1 negatively impacted v-Src and Slf2 activity compared with the FNIPs, which enhanced v-Src and Slf2 activity (Figure 3A). One possible explanation for the observed differences in FNIPs' and Tsc1's impact on kinase clients is that the FNIPs, but not Tsc1, interact with several other co-chaperones including p23 and Hop. While Hop engages the Hsp90 system early in the chaperone cycle to bridge client proteins to Hsp90 from Hsp70, p23 is considered a late-acting co-chaperone involved in the final steps of the chaperone cycle. FNIPs binding to these co-chaperones suggests they may be found throughout the entirety of the chaperone cycle, whereas Tsc1 may be a more specialized co-chaperone present only early in the Hsp90 cycle. However, due to the exquisite complexity and number of other co-chaperones, it is difficult to disentangle the exact temporal steps of FNIP1, FNIP2, and Tsc1 in the Hsp90 chaperone cycle. Notably, all three of these co-chaperones can be in complex with the co-chaperone PP5 (Woodford et al., 2016, 2017), a protein phosphatase that dephosphorylates and inactivates GR (Wang et al., 2007; Zuo et al., 1999). The Hsp90 co-chaperones FKBP51 and -52 are also specialized SHR co-chaperones that regulate SHR maturation and play a role in translocation of ligand-bound SHR to the nucleus (Guy et al., 2015; Mazaira et al., 2021; Riggs et al., 2007). While it remains unknown whether FNIPs

and Tsc1 are important for subcellular localization of SHR, the current understanding of SHR activation would suggest that all components of the complex present at the time of ligand binding localize to the nuclear membrane. Whether FNIPs and Tsc1 interact with FKBP51/52 is also unknown and may provide a clue as to the importance of FNIPs and Tsc1 in SHR translocation.

Post-translational modification (PTM) tunes Hsp90 chaperone and co-chaperone function and co-chaperone interaction. This constellation of PTM-mediated regulatory signals is collectively known as the chaperone code (Backe et al., 2020). We and others have reported PTMs of Tsc1 (Astrinidis et al., 2003; Lee et al., 2008; Li et al., 2018), FNIP1 (Manford et al., 2020; Sager et al., 2019), and PP5 (Dushukyan et al., 2017). We have also previously unraveled a CK2- and PP5-dependent mechanism that acts to titrate FNIP1 interaction with Hsp90 (Sager et al., 2019). This system is likely to be a critical determinant of GR ligand binding and maturation and potentially also the other SHRs. Further, Hsp90 itself exhibits decreased MD acetylation (residues K407/K419) in response to Tsc1 loss, and in fact, Tsc1 requires this acetylation for its interaction with Hsp90 (Woodford et al., 2019). This modification could potentially allow Hsp90 to discriminate between these specialized co-chaperone complexes, though its impact on FNIP-mediated regulation of Hsp90 function remains an open question.

Limitations of the study

It is noteworthy that we did not observe some of the common clients of Hsp90 in our FNIP1, FNIP2, or Tsc1 interactome. It is not unusual, based on previously published work, to not be able to see the established interacting proteins through mass spectrometry analysis. This could be potentially because of their nature of transient interaction. Crucially, our interactome findings revealed an interaction between FNIP1 and Tsc1 that was previously unknown. Here, we use point mutations and truncation constructs to dissect the binding mechanism for FNIP1, FNIP2, and Tsc1 to Hsp90 and each other. Most of these mutants have been previously characterized and are known to properly fold; however, there is still the possibility that some of the results presented here could be affected by misfolding or altered conformation of mutant or truncated proteins.

STAR★METHODS

RESOURCE AVAILABILITY

Lead contact—Further information and requests for resources and reagents should be directed to and will be fulfilled by the lead contact, Mehdi Mollapour (mollapom@upstate.edu).

Materials availability—Plasmids generated in this study will be made available on request, but we may require a payment and/or a completed materials transfer agreement if there is potential for commercial application.

Data and code availability—The mass spectrometry proteomics data have been deposited to the ProteomeXchange Consortium via the PRIDE (Perez-Riverol et al., 2019)

partner repository and are publicly available as of the date of publication. Accession numbers are listed in the key resources table. This paper does not report original code. Any additional information required to reanalyze the data reported in this paper is available from the lead contact upon request.

EXPERIMENTAL MODEL AND SUBJECT DETAILS

Cell lines—Cultured human embryonic kidney (HEK293) cells were grown in Dulbecco's Modified Eagle Medium (DMEM, Sigma-Aldrich) supplemented with 10% fetal bovine serum (FBS, Sigma-Aldrich). HEK293 cells were acquired from (American Type Culture Collection, ATCC). Cells were maintained in a CellQ incubator (Panasonic Healthcare) at 37°C in an atmosphere containing 5% CO₂.

Plasmids—For mammalian expression pcDNA5-FNIP1-HA and pcDNA5-FNIP1-D-HA, pcDNA3-Hsp90α truncations (Woodford et al., 2016), pcDNA3-FNIP1-FLAG and pcDNA3-FNIP1-D-FLAG (Sager et al., 2019), pcDNA3.1-Tsc1-FLAG and pcDNA3.1-Tsc1-D-FLAG (Woodford et al., 2017) constructs were cloned previously. pcDNA3-FNIP2-FLAG, pRS422-ADH-FNIP1-myc, pRS422-ADH-FNIP2-myc, pRS422-ADH-Tsc1-myc, p424-ADH-FNIP1-FLAG, p424-ADH-FNIP2-FLAG, and p424-ADH-Tsc1-FLAG were subcloned using the restriction enzymes into their respective vectors (see Table S4). The empty vectors (EV) containing these tags were used and also referred to as controls. pHCA/rGR (Garabedian and Yamamoto, 1992), constitutively expressing glucocorticoid receptor (GR) under control of the Alcohol dehydrogenase promoter (*ADHI*), the GRE reporter vector p DS26X, a *URA3* vector which expresses β-galactosidase (encoded by *lacZ*) as a reporter gene under control of a promoter bearing 3×GR response elements (Schena et al., 1989) was reported previously (Sager et al., 2019). pUCdeltaSS-ERE (Picard et al., 1990), 2x*RLM1-LacZ* reporter plasmid (Truman et al., 2006), 4XHSE-*LacZ*-pUp41a (Truman et al., 2006), and YpRS426-*GALI-v-Src* plasmid (Murphy et al., 1993) were all reported previously. pcDNA3.1-GR-FLAG and truncation constructs, p413-*GPD-V5-ERα*, and p413-*GPD-V5-AR* were synthesized by Genscript. Point mutations were made using site-directed mutagenesis (see Table S4) and confirmed by DNA sequencing.

Yeast strains—The yeast strain pp30 (*MATa*, *tp1-289*, *leu2-3,112*, *his3-200*, *ura3-52*, *ade2-101*, *lys2-801*, *hsc82KANMX4*, *hsp82KANMX4*) expressing Hsp90α-Ycplac111 as the sole Hsp90 was used in this study. These yeast strains were reported previously (Mollapour et al., 2011).

METHOD DETAILS

Yeast growth media—Yeast cells were grown on YPDA (2% (w/v) Bacto peptone, 1% yeast extract, 2% glucose, 20 mg/L adenine), YPGal (2% (w/v) Bacto peptone, 1% yeast extract, 2% galactose, 20 mg/L adenine) and YPRaf (2% (w/v) Bacto peptone, 1% yeast extract, 2% raffinose, 20 mg/L adenine). Selective growth was on dropout 2% glucose (DO) medium with appropriate amino acids (Adams et al., 1997). Medium pH was adjusted to 6.8 with NaOH before autoclaving.

Protein extraction, IP and immunoblotting—Protein extraction from both yeast and mammalian cells was carried out using methods previously described (Mollapour et al., 2010). For immunoprecipitation, mammalian cell lysates were incubated with anti-FLAG or anti-HA antibody conjugated agarose beads (Sigma) for 2 h at 4°C. Immunopellets were washed 4 times with fresh lysis buffer (20mM Tris-HCl (pH 7.4), 100 mM NaCl, 1 mM MgCl₂, 0.1% NP40, protease inhibitor cocktail (Roche), and PhosSTOP (Roche)) and eluted in 5x Laemmli buffer. Precipitated proteins were separated by SDS-PAGE and transferred to nitrocellulose membranes. Co-immunoprecipitated proteins were detected by immunoblotting with antibodies recognizing FLAG, 6x-His (ThermoFisher Scientific), Hsp90-835-16F1, GAPDH, p23 (ENZO Life Sciences), Tsc1, FLCN, GR, Myc, V5, GAPDH, Hsp90α, FNIP2, c-Src (Cell Signalling), phospho-tyrosine, v-Src (Millipore), FNIP1, FNIP2 (NCI), FNIP1 (antibodies-online.com), Aha1 (StressMarq Biosciences), HA (Roche). Secondary antibodies raised against mouse, rabbit, and rat (Cell Signaling) and goat (Santa Cruz Biotechnology) were used (See Key resources table).

Protein extraction from yeast—Yeast cells were collected from liquid culture by centrifugation and resuspended in 500μL of protein extraction buffer (20mM Tris-HCl (pH 7.4), 500 mM NaCl, 1 mM MgCl₂, protease inhibitor cocktail (Roche), and PhosSTOP (Roche)) and two pellet volumes of acid washed glass beads. To lyse the cells, tubes were agitated using a bead beater (mini-Beadbeater 8, Biospec Products, USA) for 30 s at maximum speed and then 30 s on ice. This procedure was repeated 6X followed by (10,000Xg; 5 s) to pellet the beads and unbroken cells. The supernatant was transferred to a new microfuge tube and centrifuged (10,000Xg; 10 min) to pellet insoluble aggregates. Supernatant was then transferred to a fresh microfuge.

Assays for Hsp90 client activity in yeast—Expressed v-Src protein were detected with v-Src antibody (Millipore). v-Src activity was determined by detecting tyrosine phosphorylation with 4G10 mouse anti-phosphotyrosine antibody (Millipore). β-galactosidase assay for measuring GRE-*LacZ* expression (Garabedian and Yamamoto, 1992), ERE-*LacZ* (Picard et al., 1990), HSE-*LacZ* expression (Hjorth-Sorensen et al., 2001), and RLM1-*LacZ* (Truman et al., 2006) were described previously (Mollapour et al., 2014). Note that GRE-*LacZ* reporter was also used to measure AR activity (Picard et al., 1990).

β-Galactosidase assay—Yeast cells expressing the appropriate steroid hormone receptor (*GR*, *AR*, *ER*) and their element-*Lac-Z* reporter were grown overnight to exponential phase with a cell density of 2–3×10⁶ cells per ml in 50mL of the same medium at 30°C. Then 30μM dexamethasone (Dex), 20nM Dihydrotestosterone (DHT), or 200nM β-Estradiol. was added and followed by incubation at 30°C for 2.5hr before SHE-*LacZ* activity was measured. Heat shock element (HSE)-*LacZ* expressing yeast cells were heat shock at 39°C for 40 min. Cells were collected by centrifugation (2000×g; 5 min), washed once with dH₂O, and frozen at –80°C. β-Galactosidase activity was measured as previously described (Mollapour et al., 2011). Cell lysate (10μL) was mixed with equal volume of 2X Z-buffer (60mM Na₂HPO₄, 5mM KCl, 0.5mM MgSO₄, pH adjusted to 7.0). The mixture was added to 700μL of 2mg/ml ONPG solution (O-Nitro-phenyl-β-D-galactopyranoside dissolved in 1X Z buffer) prewarmed at 30°C. The reaction was stopped by adding 500μL

of 1M Na₂CO₃. The optical density at 420nm (OD₄₂₀) of each reaction mixture was determined. The protein concentration of the lysate was determined by the BioRad assay. The β-Galactosidase activity was calculated using the following formula: Enzyme Activity = 1000×OD₄₂₀/minute/[10μL×protein concentration(μg/μl)].

Mass spectrometry analysis—Immunoprecipitated samples were loaded onto an SDS-PAGE gel and following Coomassie staining visible bands were manually cut into small pieces approximately 1 mm × 1 mm. The selected protein gel bands were in-gel digested with chymotrypsin and the tryptic peptides were desalted and subjected to LC-MS/MS. The mass spec data were processed by MaxQuant and proteins were identified by database searching with Uniprot human database. Data are presented in (Table S1).

Limited proteolysis coupled mass spectrometry analysis—Limited proteolysis of GR was achieved by exposing 10μg recombinant GR (0.5 μg/μL; Thermo Scientific) +/-1.0 μg recombinant Hsp90α to 2.0 μg/mL TPCK-treated trypsin (Sigma) for 6 min on ice, as previously described (Woodford et al., 2021). Digest was loaded onto an SDS-PAGE gel and following Coomassie staining visible bands were manually cut into small pieces approximately 1 mm × 1 mm. The selected protein gel bands were in-gel digested with chymotrypsin and the tryptic peptides were desalted and subjected to LC-MS/MS. The mass spec data were processed by MaxQuant and proteins were identified by database searching with Uniprot human database. Data are presented in (Table S1).

QUANTIFICATION AND STATISTICAL ANALYSIS

All statistics were performed using GraphPad Prism version 9.2.0 for macOS (GraphPad Software, La Jolla, California, USA, www.graphpad.com). Statistical significance was ascertained between individual samples using Tukey's multiple comparisons test (Table S3). Significance was denoted as asterisks in each figure: *p < 0.05; **p < 0.05; ***p < 0.005; ****p < 0.0005. Error bars represent the standard deviation (S.D.) for three independent experiments.

Supplementary Material

Refer to Web version on PubMed Central for supplementary material.

ACKNOWLEDGMENTS

We thank Dr. Giorgio Colombo (University of Pavia) and Drs. Guoan Zhang and Mengmeng Zhu (Weill Cornell) for constructive discussions. This work was partly supported by the Upstate Foundation (M.M. and D.B.) and the Carol M. Baldwin Breast Cancer Fund (M.M.). This work was also supported by the National Institute of General Medical Sciences of the National Institutes of Health under award numbers R01GM124256 (M.M.) and R35GM139584 (M.M.). The content is solely the responsibility of the authors and does not necessarily represent the official views of the National Institutes of Health.

REFERENCES

Abdou NI, Rider V, Greenwell C, Li X, and Kimler BF (2008). Fulvestrant (Faslodex), an estrogen selective receptor downregulator, in therapy of women with systemic lupus erythematosus. clinical, serologic, bone density, and T cell activation marker studies: a double-blind placebo-controlled trial. *J. Rheumatol* 35, 797. [PubMed: 18381791]

- Adams A, Gottschling DE, Kaiser CA, and Stearns T. (1997). *Methods in Yeast Genetics* (Cold Spring Harbor Laboratory Press).
- Ali MMU, Roe SM, Vaughan CK, Meyer P, Panaretou B, Piper PW, Prodromou C, and Pearl LH (2006). Crystal structure of an Hsp90-nucleotide-p23/Sba1 closed chaperone complex. *Nature* 440, 1013–1017. 10.1038/nature04716. [PubMed: 16625188]
- Astrinidis A, Senapedis W, Coleman TR, and Henske EP (2003). Cell cycle-regulated phosphorylation of hamartin, the product of the tuberous sclerosis complex 1 gene, by cyclin-dependent kinase 1/cyclin B. *J. Biol. Chem* 278, 51372–51379. 10.1074/jbc.M303956200. [PubMed: 14551205]
- Baba M, Hong SB, Sharma N, Warren MB, Nickerson ML, Iwamatsu A, Esposito D, Gillette WK, Hopkins RF 3rd, Hartley JL, et al. (2006). Folliculin encoded by the BHD gene interacts with a binding protein, FNIP1, and AMPK, and is involved in AMPK and mTOR signaling. *Proc. Natl. Acad. Sci. USA* 103, 15552–15557. 10.1073/pnas.0603781103. [PubMed: 17028174]
- Backe SJ, Sager RA, Woodford MR, Makedon AM, and Mollapour M (2020). Post-translational modifications of Hsp90 and translating the chaperone code. *J. Biol. Chem* 295, 11099–11117. 10.1074/jbc.REV120.011833. [PubMed: 32527727]
- Biendl MM, and Buchner J (2019). Structure, function, and regulation of the Hsp90 machinery. *Cold Spring Harbor Perspect. Biol* 11, a034017. 10.1101/cshperspect.a034017.
- Biendl MM, Riedl M, and Buchner J (2020). Hsp90 Co-chaperones form plastic genetic networks adapted to client maturation. *Cell Rep.* 32, 108063. 10.1016/j.celrep.2020.108063. [PubMed: 32846121]
- Binart N, Lombès M, and Baulieu EE (1995). Distinct functions of the 90 kDa heat-shock protein (hsp90) in oestrogen and mineralocorticosteroid receptor activity: effects of hsp90 deletion mutants. *Biochem. J* 311, 797–804. 10.1042/bj3110797. [PubMed: 7487934]
- Bresnick EH, Sanchez ER, and Pratt WB (1988). Relationship between glucocorticoid receptor steroid-binding capacity and association of the Mr 90, 000 heat shock protein with the unliganded receptor. *J. Steroid Biochem* 30, 267–269. 10.1016/0022-4731(88)90104-5. [PubMed: 3386251]
- Bresnick EH, Dalman FC, Sanchez ER, and Pratt WB (1989). Evidence that the 90-kDa heat shock protein is necessary for the steroid binding conformation of the L cell glucocorticoid receptor. *J. Biol. Chem* 264, 4992–4997. 10.1016/s0021-9258(18)83689-4. [PubMed: 2647745]
- Chen S, and Smith DF (1998). Hop as an adaptor in the heat shock protein 70 (Hsp70) and hsp90 chaperone machinery. *J. Biol. Chem* 273, 35194–35200. 10.1074/jbc.273.52.35194. [PubMed: 9857057]
- Chen S, Prapapanich V, Rimerman RA, Honore B, and Smith DF (1996). Interactions of p60, a mediator of progesterone receptor assembly, with heat shock proteins hsp90 and hsp70. *Mol. Endocrinol* 10, 682–693. 10.1210/me.10.6.682. [PubMed: 8776728]
- Cox MB, and Johnson JL (2011). The role of p23, hop, immunophilins, and other Co-chaperones in regulating Hsp90 function. *Methods Mol. Biol* 787, 45–66. 10.1007/978-1-61779-295-3_4. [PubMed: 21898226]
- Crawford ED, Schellhammer PF, McLeod DG, Moul JW, Higano CS, Shore N, Denis L, Iversen P, Eisenberger MA, and Labrie F (2018). Androgen receptor targeted treatments of prostate cancer: 35 Years of progress with antiandrogens. *J. Urol* 200, 956–966. 10.1016/j.juro.2018.04.083. [PubMed: 29730201]
- Dean ME, and Johnson JL (2021). Human Hsp90 cochaperones: perspectives on tissue-specific expression and identification of cochaperones with similar in vivo functions. *Cell Stress Chaperones* 26, 3–13. 10.1007/s12192-020-01167-0. [PubMed: 33037995]
- Dittmar KD, Demady DR, Stancato LF, Krishna P, and Pratt WB (1997). Folding of the glucocorticoid receptor by the heat shock protein (hsp) 90-based chaperone machinery. The role of p23 is to stabilize receptor.hsp90 heterocomplexes formed by hsp90.p60.hsp70. *J. Biol. Chem* 272, 21213–21220. 10.1074/jbc.272.34.21213. [PubMed: 9261129]
- Dushukyan N, Dunn DM, Sager RA, Woodford MR, Loisel DR, Daneshvar M, Baker-Williams AJ, Chisholm JD, Truman AW, Vaughan CK, et al. (2017). Phosphorylation and ubiquitination regulate protein phosphatase 5 activity and its prosurvival role in kidney cancer. *Cell Rep.* 21, 1883–1895. 10.1016/j.celrep.2017.10.074. [PubMed: 29141220]

- Edman K, Hosseini A, Bjursell MK, Aagaard A, Wissler L, Gunnarsson A, Kaminski T, Köhler C, Bäckström S, Jensen TJ, et al. (2015). Ligand binding mechanism in steroid receptors: from conserved plasticity to differential evolutionary constraints. *Structure* 23, 2280–2290. 10.1016/j.str.2015.09.012. [PubMed: 26602186]
- Eisele F, Eisele-Bürger AM, Hao X, Berglund LL, Höög JL, Liu B, and Nyström T (2021). An Hsp90 co-chaperone links protein folding and degradation and is part of a conserved protein quality control. *Cell Rep.* 35, 109328. 10.1016/j.celrep.2021.109328. [PubMed: 34192536]
- Fang Y, Fliiss AE, Robins DM, and Caplan AJ (1996). Hsp90 regulates androgen receptor hormone binding affinity in vivo. *J. Biol. Chem* 271, 28697–28702. 10.1074/jbc.271.45.28697. [PubMed: 8910505]
- Fang L, Ricketson D, Getubig L, and Darimont B (2006). Unliganded and hormone-bound glucocorticoid receptors interact with distinct hydrophobic sites in the Hsp90 C-terminal domain. *Proc. Natl. Acad. Sci. USA* 103, 18487–18492. 10.1073/pnas.0609163103. [PubMed: 17130446]
- Garabedian MJ, and Yamamoto KR (1992). Genetic dissection of the signaling domain of a mammalian steroid receptor in yeast. *Mol. Biol. Cell* 3, 1245–1257. 10.1091/mbc.3.11.1245. [PubMed: 1457829]
- Guy NC, Garcia YA, Sivils JC, Galigniana MD, and Cox MB (2015). Functions of the hsp90-binding FKBP immunophilins. *Sub Cell. Biochem* 78, 35–68. 10.1007/978-3-319-11731-7_2.
- Hainzl O, Lapina MC, Buchner J, and Richter K (2009). The charged linker region is an important regulator of Hsp90 function. *J. Biol. Chem* 284, 22559–22567. 10.1074/jbc.m109.031658. [PubMed: 19553666]
- Harris SF, Shiao AK, and Agard DA (2004). The crystal structure of the carboxy-terminal dimerization domain of htpG, the *Escherichia coli* Hsp90, reveals a potential substrate binding site. *Structure* 12, 1087–1097, S0969212604001261 [pii]. 10.1016/j.str.2004.03.020. [PubMed: 15274928]
- Hasumi H, Baba M, Hong SB, Hasumi Y, Huang Y, Yao M, Valera VA, Linehan WM, and Schmidt LS (2008). Identification and characterization of a novel folliculin-interacting protein FNIP2. *Gene* 415, 60–67. 10.1016/j.gene.2008.02.022. [PubMed: 18403135]
- Heery DM, Kalkhoven E, Hoare S, and Parker MG (1997). A signature motif in transcriptional co-activators mediates binding to nuclear receptors. *Nature* 387, 733–736. 10.1038/42750. [PubMed: 9192902]
- Hjorth-Sørensen B, Hoffmann ER, Lissin NM, Sewell AK, and Jakobsen BK (2001). Activation of heat shock transcription factor in yeast is not influenced by the levels of expression of heat shock proteins. *Mol. Microbiol* 39, 914–923, mmi2279 [pii]. 10.1046/j.1365-2958.2001.02279.x. [PubMed: 11251812]
- Hu J, Zacharek S, He YJ, Lee H, Shumway S, Duronio RJ, and Xiong Y (2008). WD40 protein FBW5 promotes ubiquitination of tumor suppressor TSC2 by DDB1-CUL4-ROC1 ligase. *Genes Dev.* 22, 866–871. 10.1101/gad.1624008. [PubMed: 18381890]
- Huang J, and Manning BD (2008). The TSC1-TSC2 complex: a molecular switchboard controlling cell growth. *Biochem. J* 412, 179–190. 10.1042/BJ20080281.
- Johnson JL, and Toft DO (1994). A novel chaperone complex for steroid receptors involving heat shock proteins, immunophilins, and p23. *J. Biol. Chem* 269, 24989–24993. 10.1016/s0021-9258(17)31487-4. [PubMed: 7929183]
- Kaziales A, Rührnöbl F, and Richter K (2021). Glucocorticoid resistance conferring mutation in the C-terminus of GR alters the receptor conformational dynamics. *Sci. Rep* 11, 12515. 10.1038/s41598-021-92039-9. [PubMed: 34131228]
- Kirschke E, Goswami D, Southworth D, Griffin PR, and Agard DA (2014). Glucocorticoid receptor function regulated by coordinated action of the Hsp90 and Hsp70 chaperone cycles. *Cell* 157, 1685–1697. 10.1016/j.cell.2014.04.038. [PubMed: 24949977]
- Koorneef LL, Kroon J, Viho EMG, Wahl LF, Heckmans KML, van Dorst MMAR, Hoekstra M, Houtman R, Hunt H, and Meijer OC (2020). The selective glucocorticoid receptor antagonist CORT125281 has tissue-specific activity. *J. Endocrinol* 246, 79–92. 10.1530/JOE-19-0486. [PubMed: 32369774]

- Lee DF, Kuo HP, Chen CT, Wei Y, Chou CK, Hung JY, Yen CJ, and Hung MC (2008). IKKbeta suppression of TSC1 function links the mTOR pathway with insulin resistance. *Int. J. Mol. Med* 22, 633–638. 10.3892/ijmm_00000065. [PubMed: 18949383]
- Li Z, Kong Y, Song L, Luo Q, Liu J, Shao C, Hou X, and Liu X (2018). Plk1-Mediated phosphorylation of TSC1 enhances the efficacy of rapamycin. *Cancer Res.* 78, 2864–2875. 10.1158/0008-5472.CAN-17-3046. [PubMed: 29559472]
- Lorenz OR, Freiburger L, Rutz DA, Krause M, Zierer BK, Alvira S, Cuéllar J, Valpuesta JM, Madl T, Sattler M, and Buchner J (2014). Modulation of the Hsp90 chaperone cycle by a stringent client protein. *Mol. Cell* 53, 941–953. 10.1016/j.molcel.2014.02.003. [PubMed: 24613341]
- MacGregor JI, and Jordan VC (1998). Basic guide to the mechanisms of antiestrogen action. *Pharmacol. Rev* 50, 151–196. [PubMed: 9647865]
- Manford AG, Rodríguez-Pérez F, Shih KY, Shi Z, Berdan CA, Choe M, Titov DV, Nomura DK, and Rape M (2020). A cellular mechanism to detect and alleviate reductive stress. *Cell* 183, 46–61.e21. 10.1016/j.cell.2020.08.034. [PubMed: 32941802]
- Mazaira GI, Echeverría PC, Ciucci SM, Monte M, Gallo LI, Erlejman AG, and Galigniana MD (2021). Differential regulation of the glucocorticoid receptor nucleocytoplasmic shuttling by TPR-domain proteins. *Biochim. Biophys. Acta Mol. Cell Res* 1868, 119000. 10.1016/j.bbamcr.2021.119000. [PubMed: 33675851]
- Meyer P, Prodromou C, Liao C, Hu B, Mark Roe S, Vaughan CK, Vlasic I, Panaretou B, Piper PW, and Pearl LH (2004). Structural basis for recruitment of the ATPase activator Aha1 to the Hsp90 chaperone machinery. *EMBO J.* 23, 511–519, [pii]. 10.1038/sj.emboj.7600060. [PubMed: 14739935]
- Moessmer P, Suren T, Majdic U, Dahiya V, Rutz D, Buchner J, and Rief M (2022). Active unfolding of the glucocorticoid receptor by the Hsp70/Hsp40 chaperone system in single-molecule mechanical experiments. *Proc. Natl. Acad. Sci. USA* 119, e2119076119. 10.1073/pnas.2119076119. [PubMed: 35377810]
- Mollapour M, Bourboulia D, Beebe K, Woodford MR, Polier S, Hoang A, Chelluri R, Li Y, Guo A, Lee MJ, et al. (2014). Asymmetric hsp90 N domain SUMOylation recruits Aha1 and ATP-competitive inhibitors. *Mol. Cell* 53, 317–329. 10.1016/j.molcel.2013.12.007. [PubMed: 24462205]
- Mollapour M, Tsutsumi S, Donnelly AC, Beebe K, Tokita MJ, Lee MJ, Lee S, Morra G, Bourboulia D, Scroggins BT, et al. (2010). Swe1Wee1-dependent tyrosine phosphorylation of Hsp90 regulates distinct facets of chaperone function. *Mol. Cell* 37, 333–343, S1097-2765(10)00030-4 [pii]. 10.1016/j.molcel.2010.01.005. [PubMed: 20159553]
- Mollapour M, Tsutsumi S, Truman AW, Xu W, Vaughan CK, Beebe K, Konstantinova A, Vourganti S, Panaretou B, Piper PW, et al. (2011). Threonine 22 phosphorylation attenuates hsp90 interaction with cochaperones and affects its chaperone activity. *Mol. Cell* 41, 672–681, S1097-2765(11)00094-3 [pii]. 10.1016/j.molcel.2011.02.011. [PubMed: 21419342]
- Murphy SM, Bergman M, and Morgan DO (1993). Suppression of c-Src activity by C-terminal Src kinase involves the c-Src SH2 and SH3 domains: analysis with *Saccharomyces cerevisiae*. *Mol. Cell Biol* 13, 5290–5300. 10.1128/mcb.13.9.5290-5300.1993. [PubMed: 7689149]
- Murphy PJ, Morishima Y, Chen H, Galigniana MD, Mansfield JF, Simons SS Jr., and Pratt WB (2003). Visualization and mechanism of assembly of a glucocorticoid receptor.Hsp70 complex that is primed for subsequent Hsp90-dependent opening of the steroid binding cleft. *J. Biol. Chem* 278, 34764–34773, [pii]. 10.1074/jbc.m304469200. [PubMed: 12807878]
- Nathan DF, and Lindquist S (1995). Mutational analysis of Hsp90 function: interactions with a steroid receptor and a protein kinase. *Mol. Cell Biol* 15, 3917–3925. 10.1128/mcb.15.7.3917. [PubMed: 7791797]
- Panaretou B, Prodromou C, Roe SM, O'Brien R, Ladbury JE, Piper PW, and Pearl LH (1998). ATP binding and hydrolysis are essential to the function of the Hsp90 molecular chaperone in vivo. *EMBO J.* 17, 4829–4836. 10.1093/emboj/17.16.4829. [PubMed: 9707442]
- Panaretou B, Siligardi G, Meyer P, Maloney A, Sullivan JK, Singh S, Millson SH, Clarke PA, Naaby-Hansen S, Stein R, et al. (2002). Activation of the ATPase activity of hsp90 by the stress-regulated cochaperone aha1. *Mol. Cell* 10, 1307–1318, S1097276502007852 [pii]. 10.1016/s1097-2765(02)00785-2. [PubMed: 12504007]

- Perez-Riverol Y, Csordas A, Bai J, Bernal-Llinares M, Hewapathirana S, Kundu DJ, Inuganti A, Griss J, Mayer G, Eisenacher M, et al. (2019). The PRIDE database and related tools and resources in 2019: improving support for quantification data. *Nucleic Acids Res.* 47, D442–D450. 10.1093/nar/gky1106. [PubMed: 30395289]
- Picard D, Khursheed B, Garabedian MJ, Fortin MG, Lindquist S, and Yamamoto KR (1990). Reduced levels of hsp90 compromise steroid receptor action in vivo. *Nature* 348, 166–168. 10.1038/348166a0. [PubMed: 2234079]
- Piper PW, Panaretou B, Millson SH, Trumana A, Mollapour M, Pearl LH, and Prodromou C (2003). Yeast is selectively hypersensitized to heat shock protein 90 (Hsp90)-targeting drugs with heterologous expression of the human Hsp90 β , a property that can be exploited in screens for new Hsp90 chaperone inhibitors. *Gene* 302, 165–170, S0378111902011022 [pii]. 10.1016/S0378-1119(02)01102-2. [PubMed: 12527207]
- Pratt WB (1987). Transformation of glucocorticoid and progesterone receptors to the DNA-binding state. *J. Cell. Biochem* 35, 51–68. 10.1002/jcb.240350105. [PubMed: 3312247]
- Pratt WB, and Toft DO (2003). Regulation of signaling protein function and trafficking by the hsp90/hsp70-based chaperone machinery. *Exp. Biol. Med.* (Maywood) 228, 111–133. 10.1177/153537020322800201. [PubMed: 12563018]
- Pratt WB, Hutchison KA, and Scherrer LC (1992). Steroid receptor folding by heat-shock proteins and composition of the receptor heterocomplex. *Trends Endocrinol. Metab* 3, 326–333, 1043-2760(92)90111-D [pii]. 10.1016/1043-2760(92)90111-d. [PubMed: 18407118]
- Prodromou C (2012). The ‘active life’ of Hsp90 complexes. *Biochim. Biophys. Acta* 1823, 614–623, S0167-4889(11)00219-9 [pii]. 10.1016/j.bbamcr.2011.07.020. [PubMed: 21840346]
- Prodromou C, and Pearl LH (2003). Structure and functional relationships of Hsp90. *Curr. Cancer Drug Targets* 3, 301–323. 10.2174/1568009033481877. [PubMed: 14529383]
- Prodromou C, Roe SM, O’Brien R, Ladbury JE, Piper PW, and Pearl LH (1997). Identification and structural characterization of the ATP/ADP-binding site in the Hsp90 molecular chaperone. *Cell* 90, 65–75, S0092-8674(00)80314-1 [pii]. 10.1016/S0092-8674(00)80314-1. [PubMed: 9230303]
- Riggs DL, Cox MB, Tardif HL, Hessling M, Buchner J, and Smith DF (2007). Nuncatalytic role of the FKBP52 peptidyl-prolyl isomerase domain in the regulation of steroid hormone signaling. *Mol. Cell Biol* 27, 8658–8669. 10.1128/MCB.00985-07. [PubMed: 17938211]
- Sager RA, Woodford MR, Shapiro O, Mollapour M, and Bratslavsky G (2018). Sporadic renal angiomyolipoma in a patient with Birt-Hogg-Dubé: chaperones in pathogenesis. *Oncotarget* 9, 22220–22229. 10.18632/oncotarget.25164. [PubMed: 29774133]
- Sager RA, Woodford MR, Backe SJ, Makedon AM, Baker-Williams AJ, DiGregorio BT, Loiselle DR, Haystead TA, Zachara NE, Prodromou C, et al. (2019). Post-translational regulation of FNIP1 creates a rheostat for the molecular chaperone Hsp90. *Cell Rep.* 26, 1344–1356.e5. 10.1016/j.celrep.2019.01.018. [PubMed: 30699359]
- Sahasrabudhe P, Rohrberg J, Biebl MM, Rutz DA, and Buchner J (2017). The plasticity of the Hsp90 Co-chaperone system. *Mol. Cell* 67, 947–961.e5. 10.1016/j.molcel.2017.08.004. [PubMed: 28890336]
- Sanjabi S, Williams KJ, Sacconi S, Zhou L, Hoffmann A, Ghosh G, Gerondakis S, Natoli G, and Smale ST (2005). A c-Rel subdomain responsible for enhanced DNA-binding affinity and selective gene activation. *Genes Dev.* 19, 2138–2151. 10.1101/gad.1329805. [PubMed: 16166378]
- Savkur RS, and Burris TP (2004). The coactivator LXXLL nuclear receptor recognition motif. *J. Pept. Res* 63, 207–212. 10.1111/j.1399-3011.2004.00126.x. [PubMed: 15049832]
- Schena M, Freedman LP, and Yamamoto KR (1989). Mutations in the glucocorticoid receptor zinc finger region that distinguish interdigitated DNA binding and transcriptional enhancement activities. *Genes Dev.* 3, 1590–1601. 10.1101/gad.3.10.1590. [PubMed: 2515114]
- Schopf FH, Biebl MM, and Buchner J (2017). The HSP90 chaperone machinery. *Nat. Rev. Mol. Cell Biol* 18, 345–360. 10.1038/nrm.2017.20. [PubMed: 28429788]
- Sharma D, Kumar S, and Narasimhan B (2018). Estrogen alpha receptor antagonists for the treatment of breast cancer: a review. *Chem. Cent. J* 12, 107. 10.1186/s13065-018-0472-8. [PubMed: 30361894]

- Simons SS Jr., Sistare FD, and Chakraborti PK (1989). Steroid binding activity is retained in a 16-kDa fragment of the steroid binding domain of rat glucocorticoid receptors. *J. Biol. Chem* 264, 14493–14497. 10.1016/s0021-9258(18)71705-5. [PubMed: 2503518]
- Taipale M, Krykbaeva I, Koeva M, Kayatekin C, Westover KD, Karras GI, and Lindquist S (2012). Quantitative analysis of HSP90-client interactions reveals principles of substrate recognition. *Cell* 150, 987–1001. 10.1016/j.cell.2012.06.047. [PubMed: 22939624]
- Tang X, Chang C, Mosallaei D, Woodley DT, Schönthal AH, Chen M, and Li W (2022). Heterogeneous responses and isoform compensation the dim therapeutic window of Hsp90 ATP-binding inhibitors in cancer. *Mol. Cell Biol* 42, e0045921. 10.1128/MCB.00459-21. [PubMed: 34871064]
- Truman AW, Millson SH, Nuttall JM, King V, Mollapour M, Prodromou C, Pearl LH, and Piper PW (2006). Expressed in the yeast *Saccharomyces cerevisiae*, human ERK5 is a client of the Hsp90 chaperone that complements loss of the Slp2p (Mpk1p) cell integrity stress-activated protein kinase. *Eukaryot. Cell* 5, 1914–1924, EC.00263-06 [pii]10.1128/EC.00263-06. 10.1128/ec.00263-06. [PubMed: 16950928]
- Tsutsumi S, Mollapour M, Prodromou C, Lee CT, Panaretou B, Yoshida S, Mayer MP, and Neckers LM (2012). Charged linker sequence modulates eukaryotic heat shock protein 90 (Hsp90) chaperone activity. *Proc. Natl. Acad. Sci. USA* 109, 2937–2942, 1114414109 [pii]10.1073/pnas.1114414109. 10.1073/pnas.1114414109. [PubMed: 22315411]
- Verba KA, Wang RYR, Arakawa A, Liu Y, Shirouzu M, Yokoyama S, and Agard DA (2016). Atomic structure of Hsp90-Cdc37-Cdk4 reveals that Hsp90 traps and stabilizes an unfolded kinase. *Science* 352, 1542–1547. 10.1126/science.aaf5023. [PubMed: 27339980]
- Wang Z, Chen W, Kono E, Dang T, and Garabedian MJ (2007). Modulation of glucocorticoid receptor phosphorylation and transcriptional activity by a C-terminal-associated protein phosphatase. *Mol. Endocrinol* 21, 625–634. 10.1210/me.2005-0338. [PubMed: 17185395]
- Weikl T, Muschler P, Richter K, Veit T, Reinstein J, and Buchner J (2000). C-terminal regions of Hsp90 are important for trapping the nucleotide during the ATPase cycle. *J. Mol. Biol* 303, 583–592. 10.1006/jmbi.2000.4157. [PubMed: 11054293]
- Woodford MR, Dunn DM, Blanden AR, Capriotti D, Loiselle D, Prodromou C, Panaretou B, Hughes PF, Smith A, Ackerman W, et al. (2016). The FNIP co-chaperones decelerate the Hsp90 chaperone cycle and enhance drug binding. *Nat. Commun* 7, 12037. 10.1038/ncomms12037. [PubMed: 27353360]
- Woodford MR, Sager RA, Marris E, Dunn DM, Blanden AR, Murphy RL, Rensing N, Shapiro O, Panaretou B, Prodromou C, et al. (2017). Tumor suppressor Tsc1 is a new Hsp90 co-chaperone that facilitates folding of kinase and non-kinase clients. *EMBO J.* 36, 3650–3665. 10.15252/embj.201796700. [PubMed: 29127155]
- Woodford MR, Hughes M, Sager RA, Backe SJ, Baker-Williams AJ, Bratslavsky MS, Jacob JM, Shapiro O, Wong M, Bratslavsky G, et al. (2019). Mutation of the co-chaperone Tsc1 in bladder cancer diminishes Hsp90 acetylation and reduces drug sensitivity and selectivity. *Oncotarget* 10, 5824–5834. 10.18632/oncotarget.27217. [PubMed: 31645902]
- Woodford MR, Baker-Williams AJ, Sager RA, Backe SJ, Blanden AR, Hashmi F, Kancherla P, Gori A, Loiselle DR, Castelli M, et al. (2021). The tumor suppressor folliculin inhibits lactate dehydrogenase A and regulates the Warburg effect. *Nat. Struct. Mol. Biol* 28, 662–670. 10.1038/s41594-021-00633-2. [PubMed: 34381247]
- Zou J, Guo Y, Guettouche T, Smith DF, and Voellmy R (1998). Repression of heat shock transcription factor HSF1 activation by HSP90 (HSP90 complex) that forms a stress-sensitive complex with HSF1. *Cell* 94, 471–480, S0092-8674(00)81588-3 [pii]. 10.1016/s0092-8674(00)81588-3. [PubMed: 9727490]
- Zuo Z, Urban G, Scammell JG, Dean NM, McLean TK, Aragon I, and Honkanen RE (1999). Ser/Thr protein phosphatase type 5 (PP5) is a negative regulator of glucocorticoid receptor-mediated growth arrest. *Biochemistry* 38, 8849–8857. 10.1021/bi990842e. [PubMed: 10413457]

Highlights

- FNIP1 forms mutually exclusive functional complexes with FNIP2 and Tsc1 co-chaperones
- Hsp90 co-chaperone complexes differentially regulate client protein activity
- FNIP1/2 and Tsc1 enhance steroid hormone receptor ligand binding and activity
- Hsp90 induces structural changes in the glucocorticoid receptor ligand-binding pocket

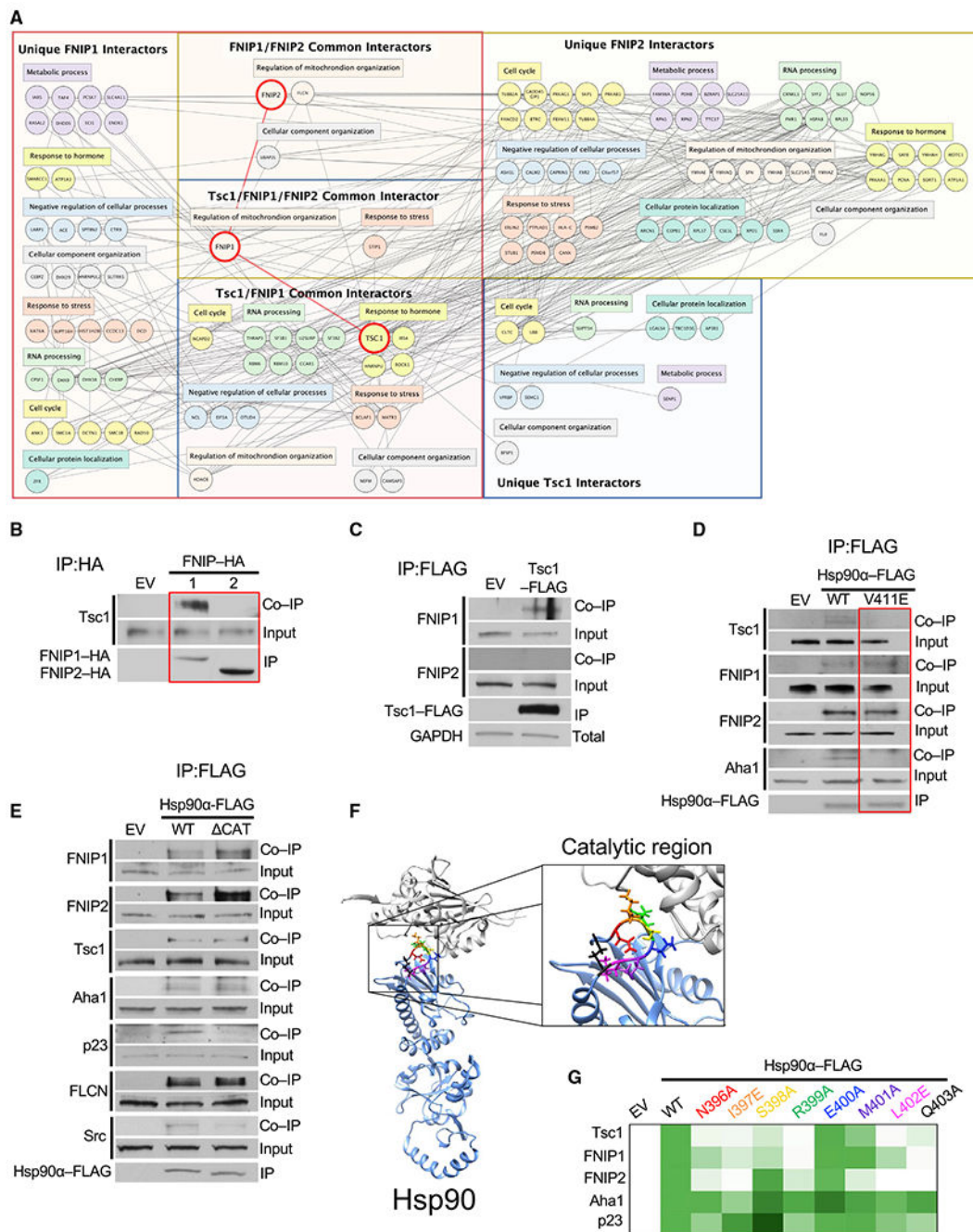


Figure 1. Hsp90 catalytic loop facilitates binding of Tsc1 and FNIPs co-chaperones
 (A) FNIP1-FLAG, FNIP2-FLAG, or Tsc1-FLAG was transiently expressed in HEK293 cells. FLAG-tagged proteins were isolated by immunoprecipitation (IP) and subject to liquid chromatography-tandem mass spectrometry (LC-MS/MS) to identify interacting proteins. Interacting proteins were divided into categories based on biological function using <https://string-db.org>. See also Figure S1.
 (B) FNIP1-HA, FNIP2-HA, or empty vector (EV; control) was immunoprecipitated from HEK293 cells. coIP of Tsc1 was examined by immunoblot.

(C) Tsc1-FLAG was immunoprecipitated from HEK293 cells. coIP of FNIP1 or FNIP2 was examined by immunoblot. GAPDH was used as a loading control.

(D) Hsp90 α -FLAG-wild type (WT) and -V411E were transiently transfected and immunoprecipitated from HEK293 cells. EV was used as a control. coIP of co-chaperones were examined by immunoblot.

(E) Full-length Hsp90 α -FLAG or Hsp90 without the catalytic loop (CAT) was expressed and immunoprecipitated from HEK293 cells. coIP of clients and co-chaperones was evaluated by immunoblot. EV was used as a control.

(F) Structure of a single Hsp90 β protomer (PDB: 5FWK) with the catalytic residues colored as follows: red, N396; orange, I397; yellow, S398; green, R399; blue, E400; purple, M401; pink, L402; black, Q403. Structures were rendered using Chimera v.1.12 (UCSF).

(G) Heatmap representation of Hsp90 α -FLAG catalytic point mutant interaction with co-chaperones. See also Figure S2.

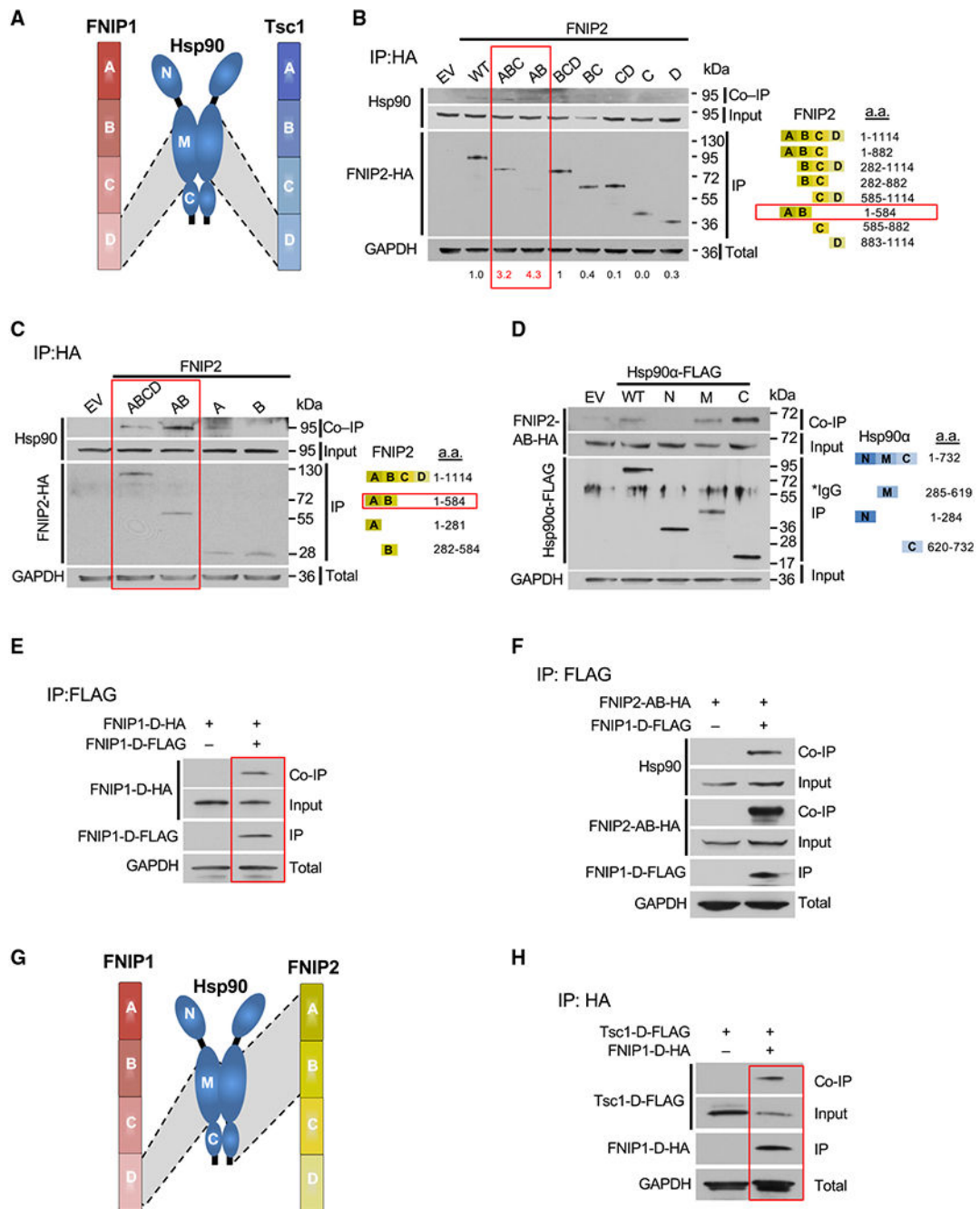


Figure 2. Architecture of FNIP2 co-chaperone association with Hsp90

(A) Schematic of FNIP1 and Tsc1 carboxy-domains (FNIP1-D, Tsc1-D) binding to the middle domain of Hsp90.

(B) Domains of FNIP2-HA were transiently expressed in HEK293 cells and isolated by IP. Endogenous Hsp90 coIP was evaluated by immunoblot. EV was used as a control. The ratio of Hsp90-coIP:FNIP2-IP was determined by densitometry.

(C) Hsp90-binding domain of FNIP2 was divided into smaller fragments, which were subsequently expressed and isolated from HEK293 cells. coIP of endogenous Hsp90 was examined by immunoblot. EV was used as a control.

(D) Hsp90 α -FLAG domains were co-transfected in HEK293 cells with FNIP2-AB-HA. Hsp90 α domains were isolated, and coIP of FNIP2-AB-HA was examined by immunoblot. EV was used as a control.

(E) FNIP1-D-HA and FNIP1-D-FLAG were co-expressed in HEK293 cells. FNIP1-D-FLAG was isolated by IP. coIP of FNIP1-D-HA was examined by immunoblot. FNIP1-D-HA transfection without FNIP1-D-FLAG was used as a control.

(F) FNIP1-D-FLAG and FNIP2-AB-HA were co-expressed in HEK293 cells. FNIP1-D-FLAG was immunoprecipitated, and coIP of FNIP2-AB-HA was evaluated by immunoblot. FNIP2-AB-HA expressed alone was used as a control.

(G) Schematic representation of FNIP1-carboxy-domain and FNIP2-amino-domain binding to Hsp90-MD or Hsp90-MD and -CTD, respectively.

(H) Tsc1-D-FLAG was transfected alone or with FNIP1-D-HA in HEK293 cells. coIP of Tsc1-D-FLAG with FNIP1-D-HA was examined by immunoblot.

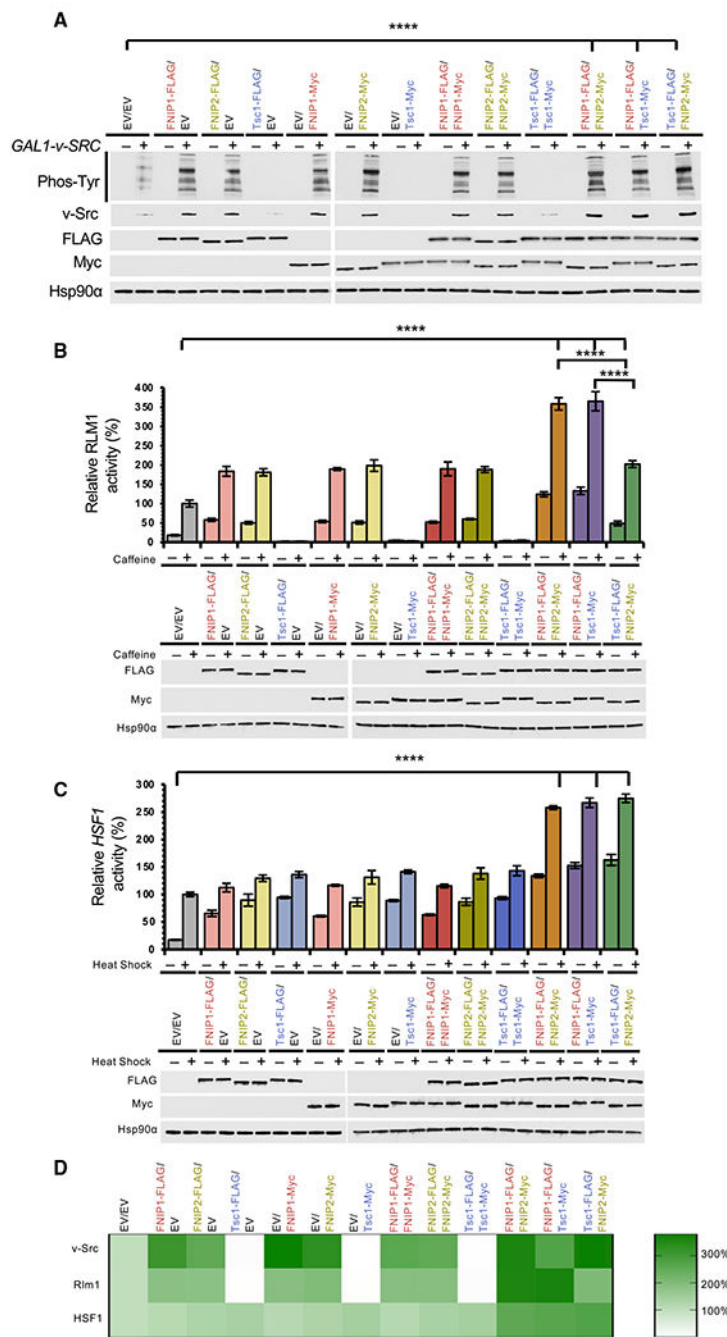


Figure 3. Differential regulation of client protein activity by FNIPs and Tsc1 co-chaperones (A) *GAL1-v-SRC* was transformed into yeast cells with human Hsp90α, containing different combinations of FNIP1-myc, FNIP1-FLAG, FNIP2-myc, FNIP2-FLAG, Tsc1-myc, or Tsc1-FLAG. Empty vector (EV) was used as a control. Cells were grown on glucose (–) or galactose (+) media. v-Src activity was examined by immunoblotting for total phosphotyrosine. v-Src, Hsp90α, and co-chaperone expression was determined by immunoblotting. v-Src activity was quantified by densitometry of total phosphotyrosine

from samples grown on galactose (+) media. Tukey's multiple comparisons test was performed to assess statistical significance (**** $p < 0.0005$).

(B) *RLM1-LacZ* activity was measured in yeast expressing human Hsp90 α and containing different combinations of FNIP1-myc, FNIP1-FLAG, FNIP2-myc, FNIP2-FLAG, Tsc1-myc, or Tsc1-FLAG. Empty vector (EV) was used as a control. Cells were grown to mid-log phase and stressed with 8 mM caffeine for 4 h. Data are presented as mean \pm standard deviation derived from three independent experiments. Tukey's multiple comparisons test was performed to assess statistical significance (**** $p < 0.0005$). Hsp90 α and co-chaperone expression was determined by immunoblotting.

(C) *HSE-LacZ* was transformed into yeast cells with human Hsp90 α and containing different combinations of FNIP1-myc, FNIP1-FLAG, FNIP2-myc, FNIP2-FLAG, Tsc1-myc, or Tsc1-FLAG. Empty vector (EV) was used as a control. Cells were heat shocked at 39°C for 40 min, and heat-shock response was measured in three independent experiments. All data represent mean \pm standard deviation (SD). Tukey's multiple comparisons test was performed to assess statistical significance (**** $p < 0.0005$). Hsp90 α and co-chaperone expression was determined by immunoblotting.

(D) Percentage of client activity (Figures 3A–3C) represented as a heatmap.

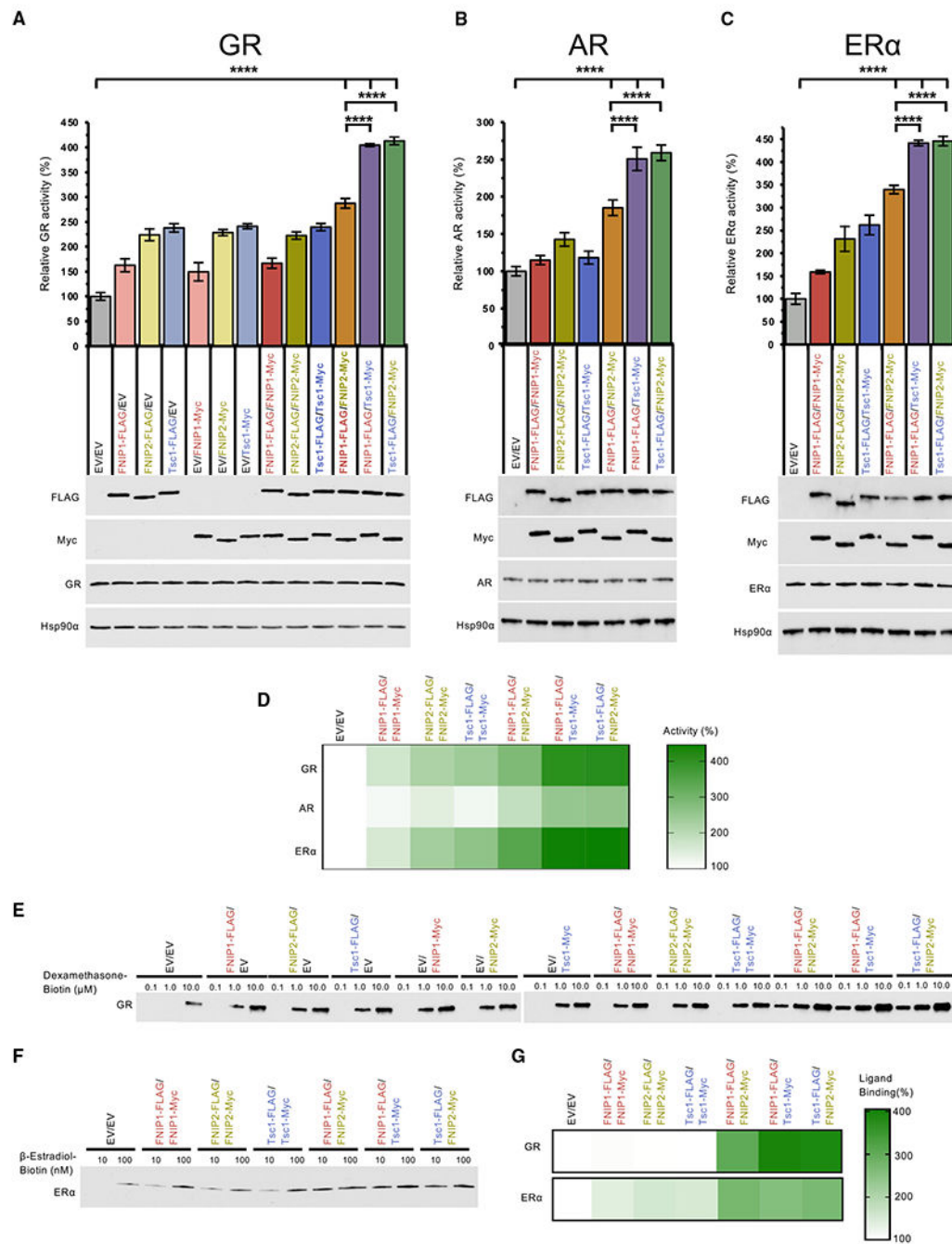


Figure 4. FNIPs and Tsc1 co-chaperones enhance the activity and ligand binding of steroid hormone receptors

(A) GR activity was measured in yeast expressing human Hsp90α and containing different combinations of FNIP1-myc, FNIP1-FLAG, FNIP2-myc, FNIP2-FLAG, Tsc1-myc, or Tsc1-FLAG. Empty vector (EV) was used as a control. Cells were grown to mid-log phase followed by the addition of 30 μM dexamethasone final concentration. Data are presented as mean ± standard deviation derived from three independent experiments. Tukey’s multiple comparisons test was performed to assess statistical significance (****p < 0.0005). Hsp90α and co-chaperone expression was determined by immunoblotting.

(B) AR activity was measured as above, using 20 nM DHT as ligand in place of dexamethasone.

(C) ER activity was measured as above, with the exception of 200 nM β -estradiol that was used in place of dexamethasone.

(D) Percentage of SHR activity (Figures 4A–4C) represented as a heatmap.

(E) Lysates from yeast expressing human GR and Hsp90 α and containing different combinations of FNIP1-myc, FNIP1-FLAG, FNIP2-myc, FNIP2-FLAG, Tsc1-myc, or Tsc1-FLAG were collected and incubated with biotinylated dexamethasone. Streptavidin-coated agarose beads were used to isolate the fraction of GR bound to the biotinylated dexamethasone. Relative GR affinity for ligand was determined by immunoblotting. Empty vector (EV) was used as a control. See also Figure S4.

(F) Lysates from yeast expressing human ER α and Hsp90 α and containing different combinations of FNIP1-myc, FNIP1-FLAG, FNIP2-myc, FNIP2-FLAG, Tsc1-myc, or Tsc1-FLAG were collected and incubated with biotinylated β -estradiol. Streptavidin-coated agarose beads were used to isolate the fraction of ER α bound to the biotinylated β -estradiol. Relative ER α affinity for ligand was determined by immunoblotting. Empty vector (EV) was used as a control. See also Figure S4.

(G) Percentage of SHR bound to ligand (Figures 4E and 4F) at the lowest ligand concentration (0.1 μ M dexamethasone-biotin, 10 nM β -estradiol-biotin) represented as a heatmap.

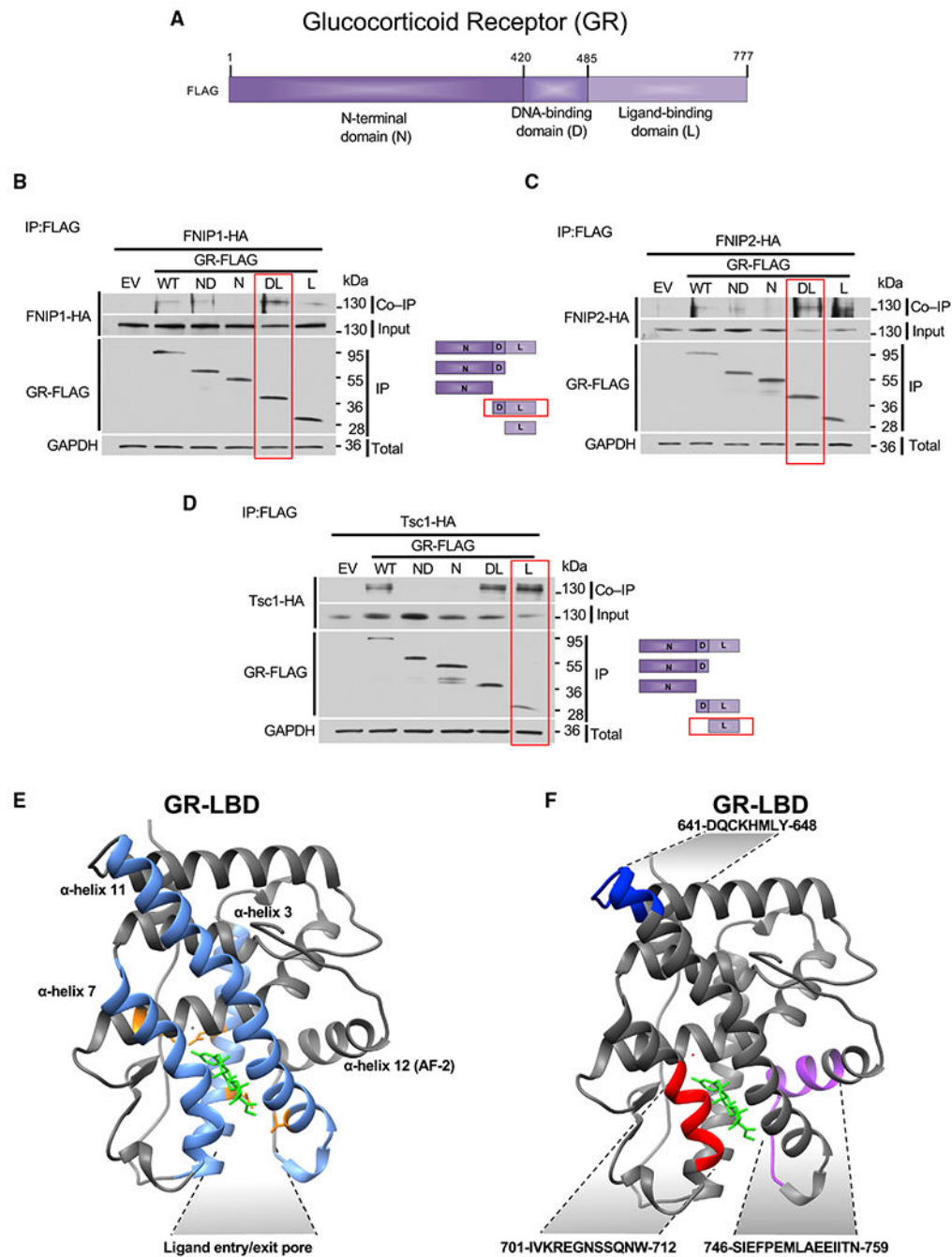


Figure 5. Hsp90 induces conformational alterations in glucocorticoid receptor ligand-binding domain

(A) Schematic representation of GR domains.

(B) GR-FLAG-WT and -domains were co-expressed with FNIP1-HA. GR domains were isolated by FLAG IP. coIP of FNIP1-HA was assessed by immunoblot. GAPDH was used as a loading control.

(C) GR-FLAG-WT and -domains were co-expressed with FNIP2-HA. GR domains were isolated by FLAG IP. coIP of FNIP2-HA was determined by immunoblot. GAPDH was used as a loading control.

(D) GR-FLAG-WT and -domains were co-expressed with Tsc1-HA. GR domains were isolated by FLAG IP. coIP of Tsc1-HA was assessed by immunoblot. GAPDH was used as a loading control.

(E) Ribbon structure of GR LBD bound to dexamethasone (PDB: 4UDC). Helices important for positioning the ligand entry/exit pore (α -helix-3, -7, -11, and -12) are colored blue. Residues that make contact with dexamethasone (Q570, N564, T739) are colored orange. Dexamethasone is colored green.

(F) Ribbon structure of GR LBD bound to dexamethasone (PDB: 4UDC) with peptides identified by LiP highlighted. Red, peptides 701–712; blue, peptides 641–648; purple, peptides 746–759. Structures were rendered using Chimera v.1.14 (UCSF).

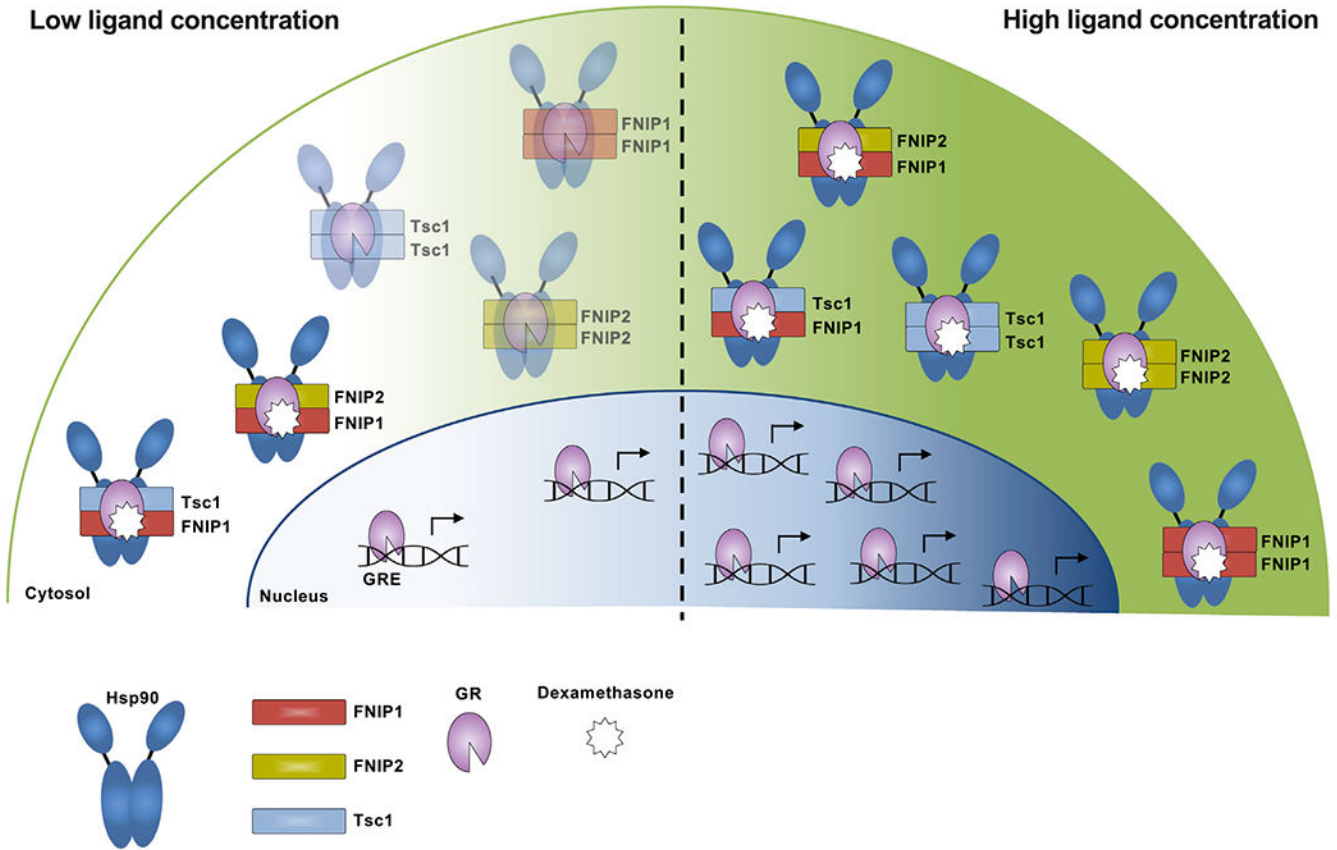


Figure 6. Hsp90:co-chaperone complexes regulate GR response to ligand

Schematic model of the cellular pool of Hsp90:co-chaperone complexes. Hsp90 exists in complex with different combinations of co-chaperones, which aid in scaffolding of clients such as GR to Hsp90. When cellular concentrations of ligand are low, only the co-chaperone complexes that promote the highest ligand-affinity client conformation allow ligand binding and subsequent activity. When excesses ligand is present, all Hsp90:co-chaperone complexes promote GR ligand binding and activity. Hsp90 is depicted as blue ovals, co-chaperones are depicted as colored rectangles (red, FNIP1; yellow, FNIP2; blue, Tsc1), GR is shown as a purple circle, and dexamethasone is depicted as white stars.

KEY RESOURCES TABLE

REAGENT or RESOURCE	SOURCE	IDENTIFIER
Antibodies		
Rabbit anti-FLAG tag	Thermo Scientific	Cat# PA1-984B; RRID:AB_347227
Rat anti-Hsp90 (16F1)	Enzo Life Sciences	Cat# ADI-SPA-835; RRID:AB_11181205
Mouse anti-GAPDH (1D4)	Enzo Life Sciences	Cat# ADI-CSA-335; RRID:AB_10617247
Rabbit anti-PP5	Cell Signaling Technology	Cat# 2289; RRID:AB_2168757
Rabbit anti-phospho-Akt S473 (D9E)	Cell Signaling Technology	Cat# 2289; RRID:AB_2315049
Mouse anti-Akt (2H10)	Cell Signaling Technology	Cat# 2967; RRID:AB_331160
Rabbit anti-GR (D6H2L)	Cell Signaling Technology	Cat# 12041; RRID:AB_2631286
Rabbit anti-HA tag (C29F4)	Cell Signaling Technology	Cat# 3724; RRID:AB_1549585
Rat anti-HA tag (3F10)	Roche	Cat# 3F10; RRID:AB_2314622
Rabbit anti-myc tag (71D10)	Cell Signaling Technology	Cat# 2278; RRID:AB_490778
Mouse anti-v-src (clone 327)	Millipore	Cat# MABS193; RRID:AB_11205595
Rabbit anti-FNIP1 (181)	NCI (Baba et al., 2006)	n/a
Rabbit anti-FNIP2 (3G)	NCI (Hasumi et al., 2008)	n/a
Rabbit anti-Tsc1 (D43E2)	Cell Signaling Technology	Cat# 6935; RRID:AB_10860420
Rat anti-Aha1 (25F2.D9)	StressMarq Biosciences	Cat# SMC-172; RRID:AB_2242422
Rabbit anti-p23	Enzo Life Sciences	Cat# ADI-SPA-670; RRID:AB_10617386
Rabbit anti-FLCN (D14G9)	Cell Signaling Technology	Cat# 3697; RRID:AB_2231646
Mouse anti-Src (L4A1)	Cell Signaling Technology	Cat# 2110; RRID:AB_10691385
Mouse anti-phospho-tyrosine (4G10)	Millipore	Cat# 05-321; RRID:AB_309678
Rabbit anti-Hsp90 α (D1A7)	Cell Signaling Technology	Cat# 8165; RRID:AB_11217436
Rabbit anti-AR (D6F11)	Cell Signaling Technology	Cat# 5153; RRID:AB_10691711
Rabbit anti-ER α (D6R2W)	Cell Signaling Technology	Cat# 13258; RRID:AB_2632959
Anti-mouse secondary	Cell Signaling Technology	Cat# 7076; RRID:AB_330924
Anti-rabbit secondary	Cell Signaling Technology	Cat# 7074; RRID:AB_2099233
Anti-rat secondary	Cell Signaling Technology	Cat# 7077; RRID:AB_10694715
Chemicals, peptides, and recombinant proteins		
Caffeine	Millipore-Sigma	Cat# C0750-500G
Dexamethasone	Millipore-Sigma	Cat# D4902
DHT	Millipore-Sigma	Cat# D-073
β -Estradiol	Millipore-Sigma	Cat# E2758
Dexamethasone-Biotin	Santa Cruz Biotech	Cat# sc-499756
β -Estradiol-Biotin	Fitzgerald Industries	Cat# 65R-AE001
Recombinant GR	ThermoFisher Scientific	Cat# A15663
Recombinant Hsp90 α	Dr. Chrisostomos Prodromou, University of Sussex	n/a
Critical commercial assays		
Mirus TransIT-2020	MirusBio	Cat# MIR5405

REAGENT or RESOURCE	SOURCE	IDENTIFIER
Anti-FLAG M2 affinity gel	Millipore-Sigma	Cat# A2220; RRID:AB_10063035
Anti-HA agarose	ThermoFisher Scientific	Cat# 26182; RRID:AB_2532162
Deposited data		
Raw and analyzed data	This paper	ProteomeXchange Consortium via the PRIDE; PDX030486
Experimental models: cell lines		
HEK293	ATCC	Cat# CRL-1573; RRID:CVCL_0045
Experimental models: organisms/strains		
PP30-Hsp90 α	(Piper et al., 2003)	n/a
Oligonucleotides		
DNA primers	Eurofins Genomics	See Table S4
Recombinant DNA		
pcDNA3-cFLAG	(Sanjabi et al., 2005)	RRID:Addgene_20011
pcDNA5-FNIP1-HA	(Baba et al., 2006)	n/a
pcDNA5-FNIP1-D-HA	(Baba et al., 2006)	n/a
pcDNA3-FNIP1-FLAG	(Sager et al., 2019)	n/a
pcDNA3-FNIP2-FLAG	This study	n/a
pcDNA5-FNIP2-HA	(Hasumi et al., 2008)	n/a
pcDNA3.1-Tsc1-FLAG	(Woodford et al., 2016)	n/a
pcDNA3-Tsc1-HA	(Hu et al., 2008)	RRID:Addgene_19911
pcDNA3.1-Tsc1-D-FLAG	(Woodford et al., 2016)	n/a
pRS422-ADH-FNIP1-myc	This study	n/a
pRS422-ADH-FNIP2-myc	This study	n/a
pRS422-ADH-Tsc1-myc	This study	n/a
p424-AHD-FNIP1-FLAG	This study	n/a
p424-AHD-FNIP2-FLAG	This study	n/a
p424-AHD-Tsc1-FLAG	This study	n/a
p413-GPD-V5-AR	This study	n/a
p413-GPD-V5-ER α	This study	n/a
pcDNA3.1 GR-FLAG	This study	n/a
p424-ADH	ATCC	Cat# 87373
pRS422-ADH	ATCC	Cat# 87479
pHCA/rGR	(Garabedian and Yamamoto, 1992)	n/a
P_DS26X	(Schena et al., 1989)	n/a
<i>2xRLM1-LacZ</i>	(Truman et al., 2006)	n/a
<i>4XHSE-LacZ</i> -pUp41a	(Truman et al., 2006)	n/a
YpRS426- <i>GAL1-v-Src</i>	(Murphy et al., 1993)	n/a
pUCdeltaSS-ERE	(Picard et al., 1990)	RRID:Addgene_108217